arXiv:1207.2722v2 [astro-ph.CO] 24 Jul 2012

Peculiar Velocity Decomposition, Redshift Space Distortion and Velocity Reconstruction in Redshift Surveys – I. The Methodology

Pengjie Zhang,[1,*] Jun Pan,[2,3] and Yi Zheng[1]
[1]*Key Laboratory for Research in Galaxies and Cosmology,*
Shanghai Astronomical Observatory, Nandan Road 80, Shanghai, 200030, China
[2]*National Astronomical Observatories, Chinese Academy of Sciences,*
20A Datun Rd., Chaoyang District, Beijing 100012, P. R. China
[3]*Purple Mountain Observatory, 2 West Beijing Rd., Nanjing 210008, P. R. China*

Massive spectroscopic surveys will measure the redshift space distortion (RSD) induced by galaxy peculiar velocity to unprecedented accuracy and open a new era of precision RSD cosmology. We develop a new method to improve the RSD modeling and to carry out robust reconstruction of the 3D large scale peculiar velocity through galaxy redshift surveys, in light of RSD. (1) We propose a mathematically unique and physically motivated decomposition of peculiar velocity into three eigen-components: an irrotational component completely correlated with the underlying density field ($\mathbf{v}_\delta$), an irrotational component uncorrelated with the density field ($\mathbf{v}_S$) and a rotational (curl) component ($\mathbf{v}_B$). The three components have different origins, different scale dependences and different impacts on RSD. (2) This decomposition has the potential to simplify and improve the RSD modeling. (I) $\mathbf{v}_B$ damps the redshift space clustering. (II) $\mathbf{v}_S$ causes an overall damping. But it also enhances the redshift space power spectrum $P^s(k,u)$ with a leading order contribution of u^4 directional dependence. Here, $u \equiv k_z/k$, k is the amplitude of the wavevector and k_z is the component along the line of sight. (III) $\mathbf{v}_\delta$ is of the greatest importance in the RSD cosmology. However, even in the limit of $\mathbf{v}_S \rightarrow 0$ and $\mathbf{v}_B \rightarrow 0$, the leading order term of $P^s(k,u)$ is $\propto (1+f\tilde{W}(k)u^2)^2$. It differs from the usual Kaiser formula by a window function $\tilde{W}(k)$. Nonlinear evolution generically drives $\tilde{W}(k) \leq 1$. We hence identify a significant systematical error causing underestimation of the structure growth parameter f by as much as $O(10\%)$ even at relatively large scale $k = 0.1h/\mathrm{Mpc}$. (IV) The velocity decomposition reveals the three origins of the finger of God (FOG) effect and suggests to simplify and improve the modeling of FOG by treating the three components separately. (V) We derive a new formula for the redshift space power spectrum. Under the velocity decomposition scheme, all high order Gaussian corrections and non-Gaussian correction of order δ^3 can be taken into account *without introducing extra model uncertainties.* (3) The velocity decomposition clarifies issues in peculiar velocity reconstruction through 3D galaxy distribution. We discuss two possible ways to fulfill the 3D $\mathbf{v}_\delta$ reconstruction. Both use the otherwise troublesome RSD in velocity reconstruction as a valuable source of information. Both have the advantage to render the reconstruction of a stochastic 3D field into the reconstruction of a deterministic window function $W^s(k,u)$ of limited degrees of freedom. Both can automatically and significantly alleviate the galaxy bias problem and, in the limit of a deterministic galaxy bias, completely overcome it. Paper I of this series of works lays out the methodology. Companion papers [1] will extensively evaluate its performance against N-body simulations.

PACS numbers: 98.80.-k; 98.80.Es; 98.80.Bp; 95.36.+x

I. INTRODUCTION

The observed galaxy clustering pattern in redshift space is modified by peculiar velocity of galaxies and shows characteristic anisotropies [2–7]. This redshift space distortion (RSD) effect provides a promising way to measure peculiar velocity at cosmological distance and makes itself a powerful probe of the dark universe. It has allowed the measurement of the structure growth rate in spectroscopic surveys such as 2dF [8, 9], SDSS [10, 11], VVDS [12], WiggleZ [13, 14] and BOSS [15, 16]. Such growth rate measurement is highly valuable in probing the nature of dark energy [17–24] and gravity [25–32]. In particular, with both the expansion rate measurement from BAO [33–36] and structure growth rate measurement from RSD, spectroscopic redshift surveys are well suited to test consistency relations in general relativity and to discriminate between dark energy and modified gravity [37]. For these reasons, RSD has become one of the key science goals of the planned stage IV dark energy projects such as the BigBOSS experiment [38] and the Euclid cosmology mission [39]. It can also be used to measure the stochastic galaxy bias [40] and the galaxy (pairwise) velocity dispersion [41], both are valuable for studying galaxy formation.

These applications heavily relies on the RSD modeling. However, modeling RSD to accuracy matching stage IV dark energy projects is very challenging, especially due to three sources of nonlinear and the associated non-Gaussianity. (1) The nonlinear mapping from real space

---

[*] Email me at: pjzhang@shao.ac.cn

clustering to redshift space clustering. Due to this nonlinearity, even the lowest order statistics in redshift space involves correlations between density and velocity fields to infinite order (e.g. [42–45]). (2) The nonlinear evolution in the real space matter density and velocity fields. (3) The nonlinear and nonlocal galaxy-matter relation. The galaxy density bias is known to have non-negligible nonlinearity and stochasticity (e.g. [46]). The galaxy velocity bias may also be needed for precision modeling (e.g. [47]). To proceed, layers of approximations and simplifications have been made.

Here we elaborate on some of these approximations/simplifications with example of matter clustering in redshift space. One of the most commonly used RSD formulae connecting the isotropic real space power spectrum $P_{\delta\delta}(k)$ to the anisotropic redshift space power spectrum $P^s_{\delta\delta}(k,u)$ is $P^s_{\delta\delta}(k,u)\simeq P_{\delta\delta}(k)(1+fu^2)^2D^{\rm FOG}(ku)$. It is a phenomenological combination and extension of the linear Kaiser effect and the finger of God (FOG) effect due to random motions. Here, $f\equiv d\ln D/d\ln a$ and $D\equiv D(z)$ is the linear density growth factor at redshift $z=1/a-1$. Throughout this paper, the superscript "s" denotes the property in redshift space. $P^s_{\delta\delta}$ depends on both k and $u\equiv k_{\parallel}/k$. Throughout the paper we adopt the z-axis as the line of sight, so $k_{\parallel}=k_z$. Approximations/simplifications made include (1) the parallel plane approximation [48], (2) linear evolution in the velocity-density relation and (3) no stochasticity between the velocity and density field [22]. (4) It also neglects most high order correlations between the density and velocity fields [43, 44]. (5) $D^{\rm FOG}(ku)$ is a phenomenological description of the FOG effect, the overall damping caused by random motion. Both a Gaussian form $D^{\rm FOG}(ku)=\exp(-(ku\sigma_v/H)^2)$ and a Lorentz form $D^{\rm FOG}(ku)=1/(1+(ku\sigma_P/H)^2/2)$ are widely adopted. However, the physical meaning of the velocity dispersion σ_v and especially the pairwise velocity dispersion σ_P is a bit ambiguous. Furthermore, deviations from the above forms have been found in simulations [49].

Various approaches have been investigated to improve the RSD modeling. A far from complete list includes the Eulerian and Lagrangian perturbation theory [42, 47, 50–56], the halo model [49, 57–60], the streaming model [4, 61, 62], the recently proposed distribution function approach [43–45] and combinations between them. Furthermore, due to significant nonlinearities involved, RSD modeling often resorts to numerical simulations on calibration and testing (e.g. [42, 49, 59, 62–65]). Despite these efforts, RSD modeling has not yet achieved the accuracy required for precision RSD cosmology. For example, recent tests against N-body simulations find that the inferred f can be biased low by $O(10\%)$ or more [63–68], significantly larger than the $O(1\%)$ statistical error in f for surveys like BigBOSS and Euclid.

Since RSD is induced by peculiar velocity, it is of crucial importance to understand the peculiar velocity field. We find that, an appropriate velocity decomposition has the potential to simplify and improve the RSD modeling. We also find that the same decomposition may enable robust reconstruction of 3D peculiar velocity in spectroscopic surveys. It has the advantage to render the otherwise troublesome RSD in velocity reconstruction into valuable source of information. The current paper aims to lay out the methodology of the proposed velocity decomposition, RSD modeling and 3D velocity reconstruction. Extensive tests against simulations and mock catalogs are required to clarify/justify/quantify numerous technical issues. These numerical results will be presented in companion papers [1].

This paper is organized as follows. In §II we decompose the peculiar velocity fields into three eigen-modes ($\mathbf{v}_\delta$, $\mathbf{v}_S$ and $\mathbf{v}_B$) and discuss related statistics. Among them, $\mathbf{v}_\delta$ is the velocity component completely correlated with the density distribution and is the one contains most cosmological information. In §III we show that the three velocity components affect RSD in different ways and their impacts can be treated separately. We are then able to derive the exact RSD formula and, furthermore, make reasonable approximations for realistic calculation. Through this methodology, we explicitly identify a significant systematical error in RSD cosmology. §IV proposes a method to reconstruct the 3D $\mathbf{v}_\delta$ from redshift surveys and the appendix D proposes an alternative. For brevity, the above sections focus on the matter field. But these results can be extended to the galaxy field straightforwardly, as briefly discussed in §V. We further argue that the velocity reconstruction is insensitive to the galaxy bias. At the end of each sections, we list key statistics to be investigated in future works. We also prepare four appendices for technical issues.

II. PECULIAR VELOCITY DECOMPOSITION

Any vector field can be decomposed into a irrotational (gradient) part and a rotational (curl) part. Analogous to the electric and magnetic fields (and also the CMB polarization field and the cosmic shear field), we denote the first one with a subscript "E" and the later one with a subscript "B". Hence the peculiar velocity $\mathbf{v}$ can be decomposed as

$$\mathbf{v}(\mathbf{x})=\mathbf{v}_E(\mathbf{x})+\mathbf{v}_B(\mathbf{x})\ . \quad (1)$$

By definition, $\nabla\times\mathbf{v}_E=0$ and $\nabla\cdot\mathbf{v}_B=0$. In Fourier space, we have $\mathbf{v}_E(\mathbf{k})=[\mathbf{v}(\mathbf{k})\cdot\hat{\mathbf{k}}]\hat{\mathbf{k}}$ and $\mathbf{v}_B(\mathbf{k})=\mathbf{v}(\mathbf{k})-\mathbf{v}_E(\mathbf{k})$.

$\mathbf{v}_E$ can be completely described by its divergence $\theta(\mathbf{x})\equiv-\nabla\cdot\mathbf{v}(\mathbf{x})/H\equiv-\nabla\cdot\mathbf{v}_E(\mathbf{x})/H$. To conveniently describe the velocity-density relation, we carry out a further decomposition,

$$\mathbf{v}_E(\mathbf{x})=\mathbf{v}_\delta(\mathbf{x})+\mathbf{v}_S(\mathbf{x})\ \ . \quad (2)$$

Both $\mathbf{v}_\delta$ and $\mathbf{v}_S$ are irrotational ($\nabla\times\mathbf{v}_\delta=0$ and $\nabla\times\mathbf{v}_S=0$). We require that $\theta_\delta\equiv-\nabla\cdot\mathbf{v}_\delta/H$ is completely correlated with the overdensity δ. So we denote this component with a subscript "δ". In Fourier space, we then have

$$\theta_\delta(\mathbf{k}) = \delta(\mathbf{k}) W(\mathbf{k}) \ , \tag{3}$$

where $W(\mathbf{k})$ is a deterministic function of $\mathbf{k}$, to be determined later immediately.

On the other hand, we require that $\theta_S \equiv -\nabla \cdot \mathbf{v}_S/H$ is uncorrelated with δ ($\langle \theta_S(\mathbf{x})\delta(\mathbf{x}+\mathbf{r})\rangle = 0$). θ_S is the source of stochasticity in the δ-θ relation, so we denote this component with a subscript "S".

We define the power spectrum between field A and field B through $\langle A(\mathbf{k})B(\mathbf{k}^{'})\rangle \equiv (2\pi)^3\delta_{3D}(\mathbf{k}+\mathbf{k}^{'})P_{AB}(\mathbf{k})$. We often use the notation $\Delta^2_{AB} \equiv k^3 P_{AB}/(2\pi^2)$, which enters into the ensemble average $\langle A(\mathbf{x})B(\mathbf{x})\rangle = \int \Delta^2_{AB}(k)dk/k$. Through the relation $\langle \delta(\mathbf{k}^{'})\theta(\mathbf{k})\rangle = \langle \delta(\mathbf{k}^{'})\theta_\delta(\mathbf{k})\rangle = \langle \delta(\mathbf{k}^{'})\delta(\mathbf{k})\rangle W(\mathbf{k})$, we obtain

$$W(\mathbf{k}) = W(k) = \frac{P_{\delta\theta}(k)}{P_{\delta\delta}(k)} \ . \tag{4}$$

Notice that, due to the isotropy of the universe, $P_{\delta\theta}(\mathbf{k}) = P_{\delta\theta}(k)$ and $P_{\delta\delta}(\mathbf{k}) = P_{\delta\delta}(k)$. So W does not depend on the direction of $\mathbf{k}$.

Hence we prove that the velocity decomposition into $\mathbf{v}_\delta$, $\mathbf{v}_S$ and $\mathbf{v}_B$ is mathematically unique, with no assumptions on the underlying density and velocity field. But the decomposition has strong physical motivation too. The three components are associated with different physical processes in the structure formation. We now proceed to their physical meanings.

A. The $\mathbf{v}_\delta$ field

In the limit $k \ll k_{\rm NL}$, $\mathbf{v}_\delta$ is the only velocity component. Here $k_{\rm NL}$ is the nonlinear scale, defined through $\Delta^2_{\delta\delta}(k_{\rm NL}) = 1$. $\mathbf{v}_B$ is a decay mode before shell crossing so it is negligible in the linear regime [69, 70]. On the other hand, in the limit $k \ll k_{\rm NL}$, $\mathbf{v}_E$ is completely correlated with the density field, with a deterministic relation $\theta = f\delta$. So $\mathbf{v}_S$ vanishes too. $\mathbf{v}_\delta$, being the most linear velocity component, is of the greatest interest to cosmology.

Nevertheless, nonlinear evolution leaves non-negligible imprints in the $\mathbf{v}_\delta$ field. A crucial point is that nonlinear evolution affects the density field and the velocity field in different or even opposite ways (e.g. [42, 69]). The third order Eulerian perturbation shows that, when the effective power index $n_{\rm eff} \gtrsim -1.9$, nonlinear evolution actually suppresses the velocity growth, while enhances the overdensity growth (Fig. 12, [69]). Even for $n_{\rm eff} \lesssim -1.9$, θ grows more slowly than the overdensity (Fig. 12, [69]). Furthermore, nonlinear evolution generates a stochastic velocity component $\mathbf{v}_S$, further reducing θ_δ with respect to δ. In the deeply nonlinear regime, after many orbit crossings, the velocity field eventually loses its correlation with the density field and we expect $\mathbf{v}_\delta \to 0$.

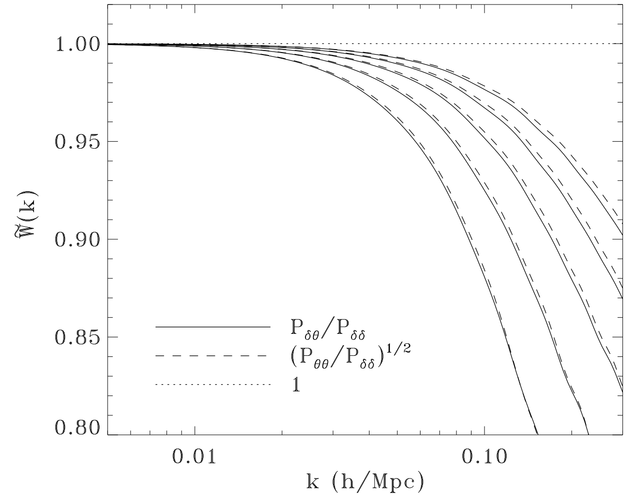

FIG. 1: Solid lines are $\tilde{W}(k,z)$ predicted by the third order Eulerian perturbation theory at redshift $z = 0.0, 0.5, 1.0, 1.5, 2.0$ (bottom up). We adopt a flat ΛCDM cosmology with $\Omega_m = 0.26$, $\Omega_b = 0.044$, $\Omega_\Lambda = 0.74$, $h = 0.71$, $\sigma_8 = 0.8$ and $n_s = 1$. Nonlinearity drives $\tilde{W}$ down from unity. Later we will show that what inferred from redshift space distortion is $f\tilde{W}$. So the structure growth rate f can be biased low by $O(10\%)$, consistent with recent findings (e.g. [63–68]). To demonstrate the $\mathbf{v}_S$ component, we also plot $\sqrt{P_{\theta\theta}/P_{\delta\delta}}$, normalized to unity at $k \to 0$ (dash lines). $\sqrt{P_{\theta\theta}/P_{\delta\delta}} = P_{\delta\theta}/P_{\delta\delta} \times \sqrt{1+\eta}$. $\eta \equiv P_{\theta_S\theta_S}/P_{\theta_\delta\theta_\delta}$ quantifies the relative amplitude of $\mathbf{v}_S$ with respect to the velocity component $\mathbf{v}_\delta$. It also quantifies the velocity divergence-density stochasticity (Eq. 7). In the limit $k \to 0$, $\eta \to 0$ and $\sqrt{P_{\theta\theta}/P_{\delta\delta}} \to P_{\delta\theta}/P_{\delta\delta}$. The nonlinear evolution generates $\mathbf{v}_S$ and causes the two sets of curves to deviate from each other. Since the third order Eulerian perturbation theory has limited range of applicability, numerical results shown in this plot are mainly presented to demonstrate the major impacts of the nonlinear evolution, to drive $\tilde{W}$ down from unity and to drive η up from zero. Robust quantifications of $\tilde{W}$ and η will be presented in companion papers [1].

Hence we should use Eq. 4 to describe the θ_δ-δ relation, instead of the linear relation $\theta_\delta = f\delta$. For the convenience of highlighting the deviation from the linear relation, we define the normalized $\tilde{W}$ through

$$\tilde{W}(k) \equiv \frac{W(k)}{W(k\to 0)} = \frac{P_{\delta\theta}(k)}{fP_{\delta\delta}(k)} \ . \tag{5}$$

$\tilde{W}$ calculated using the third order Eulerian perturbation theory is shown in Fig. 1. In companion papers [1] we will numerically evaluate this key quantity using high resolution N-body simulations. In the limit $k \to 0$, $\tilde{W} \to 1$ as expected. But nonlinear evolution soon drives $\tilde{W}$ to deviate $\tilde{W} < 1$. Even at relatively high redshift $z = 2$ and pretty linear scale $k = 0.1h$/Mpc, the deviation already reaches $O(1\%)$. The derivation increases towards low redshift and exceeds 10% at $z \lesssim 0.5$.

To better understand this behavior, we can express $\tilde{W}$ as

$$\tilde{W}(k)=r_{\delta\theta}(k)\sqrt{\frac{P_{\theta\theta}(k)}{f^2P_{\delta\delta}(k)}}\leq\sqrt{\frac{P_{\theta\theta}(k)}{f^2P_{\delta\delta}(k)}}\leq 1\ . \qquad (6)$$

Here, $r_{\delta\theta}(k)$ is the cross correlation coefficient between δ and θ. By definition, $r_{\delta\theta}(k)\leq 1$. Given the fact that velocity growths more slowly the density, $P_{\theta\theta}<f^2P_{\delta\delta}$. So we expect $\tilde{W}<1$ in nonlinear regime and expect that, when $k\gg k_{\rm NL}$, $r_{\delta\theta}\rightarrow 0$ and $\tilde{W}\rightarrow 0$.

The recognition of the velocity component $\mathbf{v}_\delta$ has several important applications. (1) It lays out a promising way to reconstruct the 3D peculiar velocity from 3D density distribution, which is accessible from galaxy spectroscopic redshift surveys. $\tilde{W}$ mimics a window function with a smoothing scale comparable to the nonlinear scale. It exerts on the density field and suppresses small scale inhomogeneities so that the smoothed density field provides a honest estimation on the underlying velocity field $\mathbf{v}_\delta$. One can find a similar window function exerting on the redshift space density, which is directly observable. Hence the reconstruction of the stochastic 3D vector field is simplified as the reconstruction of a deterministic window function with limited degrees of freedom. This is one of the most important applications of the velocity decomposition proposed in this paper. Later in §IV we will present more detailed investigation. (2) It simplifies the RSD modeling. Since $\tilde{W}\rightarrow 0$ toward small scales, nonlinearity and non-Gaussianity in the $\mathbf{v}_\delta$ field are significantly suppressed. (3) It identifies a severe systematical error in RSD cosmology. Later in §III C we will show that RSD is determined by $f\tilde{W}$ instead of f. If the factor $\tilde{W}$ is not included in the RSD cosmology, f will be biased low by $\sim 2\%$ at $z=2$ and $\sim 10\%$ at $z=0$, even if we restrict the analysis to $k\lesssim 0.1h$/Mpc. To our best knowledge, this is the first time such systematical error is diagnosized explicitly. This source of systematical error could explain recent findings of $O(10\%)$ underestimation in f inferred from simulated RSD data [63–68]. We will present more discussions on its cosmological implications in §III E.

B. The $\mathbf{v}_S$ field

To the opposite of $\mathbf{v}_\delta$, $\mathbf{v}_S$ vanishes in the linear regime and begins to grow due to the nonlinear evolution. For this reason, it lacks large scale power and hence its correlation length is smaller than that of $\mathbf{v}_\delta$. For the same reason, it is intrinsically non-Gaussian. Being uncorrelated to the density field, $\mathbf{v}_S$ induce stochasticities in the velocity-density relation. We have the relation

$$r_{\delta\theta}(k)\equiv\frac{P_{\delta\theta}(k)}{\sqrt{P_{\delta\delta}(k)P_{\theta\theta}(k)}}=\frac{1}{\sqrt{1+\eta(k)}}\ , \qquad (7)$$

where $\eta(k)\equiv P_{\theta_S\theta_S}(k)/P_{\theta_\delta\theta_\delta}(k)$. When $\mathbf{v}_S$ overwhelms over $\mathbf{v}_\delta$ ($\eta\gg 1$), $r_{\delta\theta}\rightarrow 0$ and the velocity field loses its correlation with the density field.

Based on the third order perturbation calculation, we find that $P_{\theta_S\theta_S}$ already reaches $\simeq 1\%$ of $P_{\theta_\delta\theta_\delta}$ (namely $\eta\simeq 1\%$) at $k=0.1h/$ Mpc and $z\lesssim 1$, as can be inferred from Fig. 1. As expected, the situation is less severe at higher redshifts. But even at $z=2$, $\eta\simeq 1\%$ at $k=0.2h$/Mpc. Hence in general, $\mathbf{v}_S$ is a non-negligible velocity component even at scales which are often considered as linear. Nevertheless, it is still subdominant to $\mathbf{v}_\delta$ at scale $k\lesssim 1h$/Mpc, as one can infer from Fig. 1 of [22], in combination with our Eq. 7. Our numerical evalulations obtain similiar results and we will present details in companion papers [1].

What cosmological information does it contain? One particularly interesting piece is likely the nature of gravity. For modified gravity models to pass the solar system tests while driving the late time cosmic acceleration, gravity must behave upon the environment (e.g. review articles [71, 72]). Such environment dependence often becomes prominent in the nonlinear regime and can significantly affects the velocity divergence (e.g. [32]). Being arising from nonlinear evolution, $\mathbf{v}_S$ would be sensitive to this smoking gun of modified gravity, making it attractive for testing gravity.

In §III we will show that the $\mathbf{v}_S$ induced RSD differs from the $\mathbf{v}_\delta$ induced RSD (§III). We argue that these differences can be used to separate the different velocity components and made *statistical* measurement of $\mathbf{v}_S$ possible.

C. The $\mathbf{v}_B$ field

$\mathbf{v}_B$ decays as long as the single fluid approximation for the dark matter distribution holds [69]. $\mathbf{v}_B$ grows only when the nonlinearity is sufficiently large that shell crossing happens. In the deeply nonlinear regime, we may even expect equi-partition in the velocity distribution and $\mathbf{v}_B$ can dominate over $\mathbf{v}_E$. So we expect that its power concentrates at even smaller scales than $\mathbf{v}_S$. Indeed, numerically studies [70] show that the power of this velocity component concentrates at small scales, with r.m.s. much smaller than that of $\mathbf{v}_E$. Our numerical evalulations obtain similiar results [1]. Later in §III A we will show that these behaviors significantly simplify the modeling of $\mathbf{v}_B$ induced RSD. For in depth study of $\mathbf{v}_B$, we refer the readers to [70] and references therein. In [1], we will present the statistics of $\mathbf{v}_B$ in the context of RSD.

D. Statistical description of the three velocity components

We are not at a position to calculate the statistics of these velocity components. Instead, we present some general discussions here and postpone any quantitative calculations in future works. First, since the three velocity components have different origins, the halo model scenario [41, 73–75] provides an unified way to describe the three components, with a number of extensions. (1) Since deviations from the linear theory prediction of the halo bulk motion have been diagnosized [76] and since it fails to describe the emergence of $\mathbf{v}_S$, a natural tool to describe the halo bulk motion is the third order perturbation. (2) Peculiar velocity has been treated as the sum of the halo bulk velocity and the random velocity inside of the virialized halos [77]. It may be extended to include the more complicated motion around the halo outskirt, which may be a significant source of $\mathbf{v}_B$ [70]. Nevertheless, treatment of $\mathbf{v}_B$ is trickier and we refer the readers to [70] for detailed discussions.

One important statistics relevant to RSD is the velocity correlation function. Due to symmetry considerations, it can be decomposed as [4]

$$\langle v_i(\mathbf{x}_1)v_j(\mathbf{x}_2)\rangle = \psi_\perp(r)\delta_{ij} + \left[\psi_\parallel(r) - \psi_\perp(r)\right]\frac{r_i r_j}{r^2} \ . \quad (8)$$

Here $\mathbf{r} \equiv \mathbf{x}_1 - \mathbf{x}_2$ is the pair seperation vector. $\psi_\parallel$ is the correlation function when both v_i and v_j are along $\mathbf{r}$. $\psi_\perp$ is the one when both velocities are perpendicular to $\mathbf{r}$.

$\psi_\parallel$ and $\psi_\perp$ are not independent. For a potential flow ($\mathbf{v}_\delta$ and $\mathbf{v}_S$), we have the textbook result [4]

$$\psi_\parallel(r) \ = \ \frac{d(r\psi_\perp(r))}{dr} \ , \quad (9)$$

$$\psi_\perp(r) \ = \ H^2\int \Delta^2_{\theta\theta}\frac{\sin(kr)}{kr}\frac{dk}{k^3} \ . \quad (10)$$

Here we have defined the velocity power spectrum through $\langle \mathbf{v}(\mathbf{k})\cdot\mathbf{v}(\mathbf{k}^{'})\rangle \equiv (2\pi)^3\delta_{3D}(\mathbf{k}+\mathbf{k}^{'})P_{vv}(k)$. Its covariance is defined as $\Delta^2_{vv} \equiv P_{vv}k^3/2\pi^2$.

For $\mathbf{v}_B$, we no longer have this relation. Using the fact that $\mathbf{v}_B$ can be expressed as the vorticity of a vector $\mathbf{A}$ ($\mathbf{v}_B = \nabla\times\mathbf{A}$), we derive the following relations,

$$\psi_\perp(r) \ = \ \psi_\parallel(r) + \frac{1}{2}r\frac{d\psi_\parallel(r)}{dr} \ , \quad (11)$$

$$\psi_\parallel(r) \ = \ \int \Delta^2_{v_Bv_B}(k)\frac{dk}{k}\frac{1}{3}\left[\frac{\sin kr}{(kr)^3} - \frac{\cos kr}{(kr)^2}\right] \ . \quad (12)$$

E. To do list

In companion papers [1], we will use N-body simulations to numerically evaluate statistics of these velocity fields. An incomplete list includes

- The power spectra $P_{v_\delta v_\delta}(k,z)$, $P_{v_Sv_S}(k,z)$ and $P_{v_Bv_B}(k,z)$. Their scale and redshift dependences are helpful to understand the impact of nonlinear evolution.
- The correlation function $\psi_{v_\delta v_\delta}(r,z)$, $\psi_{v_Sv_S}(r,z)$ and $\psi_{v_Bv_B}(r,z)$, of the "$\parallel$" mode and the "$\perp$" mode. These statistics quantify the correlation length of the three velocity components and tell us at which separation we can treat the velocities at two positions as independent.
- The PDFs of $\mathbf{v}_\delta$, $\mathbf{v}_S$ and $\mathbf{v}_B$. The PDFs determine the overall damping (FOG) to the redshift power spectrum. We will also calculate the cumulants to quantify non-Gaussianity of hese velocity components.
- $\tilde{W}(k,z)$. As we have addressed, $\tilde{W}$ is of crucial importance in the 3D velocity reconstruction and in the RSD cosmology. Through N-body simulations, we will robustly measure its dependence on k and z. Furthermore, we want to quantify the $\tilde{W}(k,z)$-$\Delta^2_{\delta\delta}(k,z)$ relation to better understand its dependence on the nonlinearity. Especially, we want to know if it can be well approximated by a simple function with only a few parameters.

III. MODELING THE REDSHIFT SPACE DISTORTION

Now we proceed to the RSD modeling with the aid of the proposed velocity decomposion. Following [42], we utilize the matter conservation ($(1+\delta^s(\mathbf{x}^s))d^3\mathbf{x}^s = (1+\delta(\mathbf{x}))d^3\mathbf{x}$) to derive

$$\delta^s(\mathbf{k}) = \int [1+\delta(\mathbf{x})]\exp\left(i\frac{k_zv_z}{H}\right)\exp(i\mathbf{k}\cdot\mathbf{x})d^3\mathbf{x} \quad (13)$$

In the above expression, we have neglected a Dirac funtion which only shows up when $\mathbf{k} = 0$, irrelevant to our calculation. This equation adopts the plane parallel approximation and adopts the line of sight as the z-axis. It also assumes no multiple streaming. Extention to this more complicated situation can be done by the phase space distribution function approach [43–45]. Phenomenologically speaking, multiple streaming can be described by an overall damping to the redshift space power spectrum. Hence we do not expect major changes to the results presented in this paper.

The redshift space power spectrum is given by [42]

$$P^s_{\delta\delta}(\mathbf{k}) = \int \langle(1+\delta_1)(1+\delta_2)\exp\lambda\rangle\exp(-i\mathbf{k}\cdot\mathbf{r})d^3\mathbf{r} \quad (14)$$

where $\delta_i \equiv \delta(\mathbf{x}_i)$ and $\mathbf{x}_2 \equiv \mathbf{x}_1 + \mathbf{r}$. The ensemble average $\langle\cdots\rangle$ is averaged over all $\mathbf{x}_1$ with fixed $\mathbf{r}$. For brevity, we have denoted $\lambda \equiv ik_z(v_{1z} - v_{2z})/H$. We also denote $\lambda_\alpha \equiv ik_z(v_{1z,\alpha} - v_{2z,\alpha})/H$ where $\alpha = \delta, S, B$. Due to the axial symmetry along the line of sight, $P^s_{\delta\delta}$ only depends on k and u. Hereafter we often write it as $P^s_{\delta\delta}(k,u)$.

An immediate result is that $\delta^s(\mathbf{k}_\perp, k_z = 0) = \delta(\mathbf{k}_\perp, k_z = 0)$ and $P^s_{\delta\delta}(\mathbf{k}_\perp, k_z = 0) = P_{\delta\delta}(k_\perp)$. A similar relation holds for the bispectrum, $B^s_3(\mathbf{k}_1,\mathbf{k}_2,\mathbf{k}_3) = B_3(\mathbf{k}_1,\mathbf{k}_2,\mathbf{k}_3)$ when $k_{1,z} = k_{2,z} = k_{3,z} = 0$. Later we will show that these relations are very useful in RSD modeling. Notice that no such relations exist in real space. For example, $\xi^s(\mathbf{r}_\perp, r_z = 0) \neq \xi(r_\perp)$.

A. The role of $\mathbf{v}_B$

Now we will apply the velocity decomposition to Eq. 14. Since only $\mathbf{v}_\delta$ is correlated with the overdensity, Eq. 14 can be reduced to

$$\begin{aligned} P^s_{\delta\delta}(k,u) &= \int \{\langle(1+\delta_1)(1+\delta_2)\exp\lambda_\delta\rangle \\ &\times \;\; D_S(k_z,\mathbf{r})D_B(k_z,\mathbf{r})\}\exp(-i\mathbf{k}\cdot\mathbf{r})d^3\mathbf{r} \ . \end{aligned} \tag{15}$$

The two function $D_S(k_z,\mathbf{r})$ and $D_B(k_z,\mathbf{r})$ completely describe the redshift distortion caused by $\mathbf{v}_S$ and $\mathbf{v}_B$ respectively.

$$D_S(k_z,\mathbf{r}) \equiv \left\langle \exp\left(i\frac{k_z(v_{1z,R}-v_{2z,R})}{H}\right)\right\rangle \ , \tag{16}$$

$$D_B(k_z,\mathbf{r}) \equiv \left\langle \exp\left(i\frac{k_z(v_{1z,B}-v_{2z,B})}{H}\right)\right\rangle \ . \tag{17}$$

Due to the symmetry between k_z and $-k_z$, $D_{S,B}(k_z,\mathbf{r}) = D_{S,B}(|k_z|,\mathbf{r})$.

We have $D_S \leq 1$ and $D_B \leq 1$, so both $\mathbf{v}_S$ and $\mathbf{v}_B$ suppress the clustering presented by terms inside of the bracket of Eq. 15. However, $\mathbf{v}_S$ and $\mathbf{v}_B$ can have their own clusterings and hence can in principle increase the overall clustering in redshift space. We can also define a corresponding function for $\mathbf{v}_\delta$,

$$D_\delta(k_z,\mathbf{r}) \equiv \left\langle \exp\left(i\frac{k_z(v_{1z,\delta}-v_{2z,\delta})}{H}\right)\right\rangle \ . \tag{18}$$

But since $\mathbf{v}_\delta$ is correlated with the density field, its role in RSD is too complicated to be described by a single function D_δ.

In general, these functions depend on the pair separation $\mathbf{r}$, due to correlations in the corresponding velocity fields. To describe this effect, we define

$$1+\epsilon_{\delta,S,B}(\mathbf{r},k_z) \equiv \frac{D_{\delta,S,B}(k_z,\mathbf{r})}{D_{\delta,S,B}(k_z,r\rightarrow\infty)} \ . \tag{19}$$

Here, the limit $r\rightarrow\infty$ corresponds to the limit of no velocity correlation. In this limit, peculiar velocity only causes damping (FOG). Hence we denote D at this limit with a superscript "FOG",

$$\begin{aligned} D_{\delta,S,B}(k_z,r\rightarrow\infty) &\equiv D^{\rm FOG}_{\delta,S,B}(k_z) \\ &= \left|\left\langle \exp\left(i\frac{k_z v_{z,\delta,S,B}}{H}\right)\right\rangle\right|^2 \ . \end{aligned} \tag{20}$$

As discussed in §II, $\mathbf{v}_B$ arises mostly in the deeply nonlinear regime, so we expect a correlation length shorter than scales of interest for RSD cosmology. Hence we can neglect correlation in the $\mathbf{v}_B$ field. Namely, we can make the approximation

$$\epsilon_B \simeq 0 \ \ , \ \ D_B(k_z,\mathbf{r}) \simeq D^{\rm FOG}_B(k_z) \ . \tag{21}$$

Since $D^{\rm FOG}_B$ is independent of $\mathbf{r}$, Eq. 15 is simplified as

$$\begin{aligned} P^s_{\delta\delta}(k,u) &= \left\{\int \langle(1+\delta_1)(1+\delta_2)\exp\lambda_\delta\rangle \right. \\ &\left. D_S(k_z,\mathbf{r})\exp(-i\mathbf{k}\cdot\mathbf{r})d^3\mathbf{r}\right\} D^{\rm FOG}_B(k_z) \ . \end{aligned} \tag{22}$$

The damping function $D^{\rm FOG}_B$ is related to its velocity PDF through

$$\begin{aligned} \sqrt{D^{\rm FOG}_B(k_z)} &= \int_{-\infty}^{\infty}\exp\left(i\frac{k_z v_{z,B}}{H}\right)P_B(v_{z,B})dv_{z,B} \\ &= \int_{-\infty}^{\infty}\cos\left(\frac{k_z v_{z,B}}{H}\right)P_B(v_{z,B})dv_{z,B} \ . \end{aligned}$$

Through the cumulant expansion theorem, we can express $D^{\rm FOG}_B$ in cumulants of $v_{z,B}$. The cumulant expansion theorem states that

$$\begin{aligned} \left\langle\exp\left(i\frac{k_z v}{H}\right)\right\rangle &= \exp\left(\sum_{n=1}^{\infty}\left(\frac{ik_z}{H}\right)^n\frac{\langle v^n\rangle_c}{n!}\right) \\ = \exp\left(-\frac{k_z^2\sigma_v^2}{2H^2}\right) &\exp\left(\sum_{j\geq 2}(-1)^j\left(\frac{k_z\sigma_v}{H}\right)^{2j}\frac{K_{2j}}{(2j)!}\right) \\ &= \exp\left(-\frac{x}{2}\left[1-\frac{K_4}{12}x+\frac{K_6}{360}x^2+\cdots\right]\right) \ . \end{aligned} \tag{23}$$

Here, v denotes $v_{z,B}$. $\langle\cdots\rangle_c$ is the corresponding cumulant of the quantity inside of the bracket. For a Gaussian velocity distribution, we have $\langle v^j\rangle_c = 0$ for $j\geq 3$ and recover the Gaussian FOG. For non-Gaussian distribution, higher order terms show up. Since $\langle v^{2j+1}\rangle_c = 0$, only even cumulants contribute. $K_j \equiv \langle v^j\rangle_c/\sigma_v^j$ is the reduced cumulant and $x\equiv(k_z\sigma_v/H)^2$.

Non-Gaussianity in $\mathbf{v}_B$ could be significant and we may expect that high order cumulants must be included to robustly model $D^{\rm FOG}_B$. Fortunately, the reality can be much simpler due to the fact that $\mathbf{v}_B$ has small r.m.s. Its σ_v is more than a factor of 10 smaller than that of $\mathbf{v}_E$ [70]. This means that $\sigma_{v_B} \lesssim 10$ km/s even at $z=0$. Hence for the scales of interest (e.g. $k<1h$/Mpc), we have $x\lesssim 10^{-2}$. Then the $\mathbf{v}_B$ induced FOG can be well described by the following Gaussian form,

$$D^{\rm FOG}_B(k_z) \simeq \exp\left(-\frac{k_z^2\sigma^2_{v_B}}{H^2}\right) \ . \tag{24}$$

σ_{v_B} is hard to calculate from first principle, so it shall be treated as a free parameter to be fitted by the data.

B. The role of $\mathbf{v}_S$

The situation for $\mathbf{v}_S$ is more complicated. Since a significant fraction of $\mathbf{v}_S$ comes from bulk motion, $\mathbf{v}_S$ can be still correlated over $O(10)$ Mpc separation. So we are no longer able to make the approximation $\epsilon_S = 0$. Instead, we have, with the aid of the cumulant expansion theorem,

$$1+\epsilon_S(\mathbf{r},k_z) = \exp\left[\frac{k_z^2\langle v_{1z,S}v_{2z,S}\rangle}{H^2}\right] \tag{25}$$
$$\times e^{[k_z^2\langle 3v_{1z,S}^2v_{2z,S}^2-2(v_{1z,S}^3v_{2z,S}+1\leftrightarrow 2)\rangle_c/12H^4+\cdots]}$$
$$= \frac{k_z^2\langle v_{1z,S}v_{2z,S}\rangle}{H^2}+O(v_S^4)\ .$$

Due to the symmetry $v \leftrightarrow -v$, odd terms in v do not show up in the above equation. Plugging it into Eq. 22, we find that the leading order contribution to $P^s_{\delta\delta}$ is $P_{\theta_S\theta_S}u^4$ (Eq. 26), which enhances $P^s_{\delta\delta}$. Notice that, since $\mathbf{v}_S$ is uncorrelated with the density field, it does not contribute a u^2 term as $\mathbf{v}_\delta$ does. Higher order contributions come from both fourth and higher order velocity correlations (Eq. 25) and from the convolution of ϵ_S with $\langle(1+\delta_1)(1+\delta_2)\exp\lambda_\delta\rangle$ (Eq. 15). These corrections are of the order δ^4 or higher. We group all these contributions into a single function $C_S(k,u)$ (Eq. 26). Later we argue that we may be able to set $C_S=0$ in the RSD modeling.

On the other hand, $\mathbf{v}_S$ causes an overall damping, characterized by $D^{\rm FOG}_S$,

$$\sqrt{D^{\rm FOG}_S(ku)} = \int_{-\infty}^{\infty}\exp\left(i\frac{kuv_{z,S}}{H}\right)P_S(v_{z,S})dv_{z,S}$$
$$= \int_{-\infty}^{\infty}\cos\left(\frac{kuv_{z,S}}{H}\right)P_S(v_{z,S})dv_{z,S}\ .$$

Since $\mathbf{v}_S$ arises from nonlinear evolution, it is intrinsically non-Gaussian. We will check if $D^{\rm FOG}$ can be well described by the first several cumulants, with the aid of the cumulant expansion theorem (Eq. 23).

C. The role of $\mathbf{v}_\delta$

Due to coupling between the velocity and the density fields, redshift distortion induced by $\mathbf{v}_\delta$ is complicated, although analytical expression in the Gaussian limit exists [42]. In the appendix, we derive the non-Gaussian corrections (Eq. A4). In Fourier space, we have

$$P^s_{\delta\delta}(k,u) = \Big\{P_{\delta\delta}(k)(1+f\tilde{W}(k)u^2)^2+u^4P_{\theta_S\theta_S}(k)$$
$$+C_{NG}(k,u)+C_G(k,u)+C_S(k,u)\}$$
$$\times D^{\rm FOG}_\delta(ku)D^{\rm FOG}_S(ku)D^{\rm FOG}_B(ku)\ . \tag{26}$$

Here, C_G and C_{NG} are the Fourier transforms of $C_G(\mathbf{r},k_z)$ (Eq. A5) and $C_{NG}(\mathbf{r},k_z)$ (Eq. A7), respectively. C_G contains all high order corrections if the density and velocity fields are Gaussian. C_{NG} is the extra correction caused by non-Gaussianity. Both terms are consequeces of the $\mathbf{v}_\delta$-δ correlation.

$\mathbf{v}_\delta$ also causes a FOG effect, described by $D^{\rm FOG}_\delta$. $\mathbf{v}_\delta$ is largely Gaussian due to the suppression of $\tilde{W}<1$ in the nonlinear and non-Gaussian regime. However, due to the large amplitude of σ_{v_δ}, it is unclear whether we can neglect the K_4 and/or K_6 corrections. Here σ_{v_δ} is the the one dimension velocity dispersion of $\mathbf{v}_\delta$,

$$\sigma^2_{v_\delta} \equiv \langle v^2_{\delta,z}\rangle = \frac{1}{3}\int\Delta^2_{v_\delta v_\delta}(k)\frac{dk}{k} \tag{27}$$
$$= \frac{1}{3}\int\frac{H^2}{k^2}\Delta^2_{\delta\delta}(k)W^2(k)\frac{dk}{k}\ .$$

The terms C_{NG}, C_G and C_S are the sums of infinite power series of δ. To carry out realistic calculation, we need to truncate them in a reasonable way. The first line terms in the right hand side of Eq. 26 exhaust contributions of the order δ^2. It can be rewritten in a more familiar form $P_{\delta\delta}+2u^2P_{\delta\theta}+u^4P_{\theta\theta}$ (e.g. [42]) and confirmes previous results. The second line terms are higher order in δ. The leading order term of C_{NG} is $\propto\delta^3$, while those of C_G and C_S are $\propto\delta^4$. In this sense, for Eq. 26 to be complete at the order of δ^3, we can set $C_G=0$ and $C_S=0$.

But in term of the linear density δ_L, the situation is different. (1) $P_{\theta_S\theta_S}$ vanishes in the linear perturbation theory, but emerges in the second or higher order Eulerian perturbation theory. So $P_{\theta_S\theta_S}$ itself is of the order δ_L^4 and C_S is of the order δ_L^6. (2) In the Eulerian perturbation theory, leading order terms of C_G and C_{NG} are of the order δ_L^4. So up to the order δ_L^4, we can set $C_S=0$.

Hence no matter in power series of δ or in power series of δ_L, we can set $C_S=0$ when calculating the leading order corrections to the usual RSD formula. But whether or not we shall set $C_G=0$ is an issue for numerical examination.

The inclusion of C_G and C_{NG} may appear to introduce more difficulties and uncertainties to the RSD modeling. However, this is not the case. We will show that, *the inclusion of C_G and leading order terms in C_{NG} does not introduce extra degrees of freedom in the RSD modeling.* So the inclusion of these terms is capable of reducing systematical errors, without degrading cosmological parameter constraints. This is definitely a desirable property, made possible by the proposed velocity decomposition.

1. The C_G correction

C_G is an analytical (but nonlinear) function of the two point density and velocity ($\mathbf{v}_\delta$) correlation functions (Eq. A5). Since $P_{\delta\delta}$ is directly measurable from the $k_z=0$ Fourier modes in redshift surveys, C_G up to any order can be calculated strictly without introduce any extra parameters.

C_G does not contain terms of odd order in δ. So we can split C_G as $C_G(k,u)=\sum_j C_{G,2j}(k,u)$ where $j=2,3\cdots$. In reality, we may only need the leading order

$$C_{G,4}(k,u) = \int\frac{d^3\mathbf{k}_1}{(2\pi)^3}\,P_{\delta\delta}(k_1)P_{\delta\delta}(k_2)\frac{k_{1z}k_{2z}k_z^2W_1W_2}{k_1^2k_2^2}$$
$$\times\ G(\mathbf{k},\mathbf{k}_1,\mathbf{k}_2)\ . \tag{28}$$

Here, $\mathbf{k}_2 = \mathbf{k} + \mathbf{k}_1$ and $W_i \equiv W(k_i)$. The kernel G is

$$G = \frac{k_{1z}W_1/k_1^2}{k_{2z}W_2/k_2^2} - 1 + \frac{2k_{1z}k_zW_1}{k_1^2} + \frac{k_{1z}k_{2z}k_z^2W_1W_2}{2k_1^2k_2^2} \ . \quad (29)$$

With $P_{\delta\delta}$ an observable and W a function to be fitted anyway, calculating C_G requires no extra free parameters and hence does not induce new model uncertainties.

2. The C_{NG} correction

$C_{NG}(k,u) = \sum_{j\geq 3} C_{NG,j}(k,u)$ contains connected part of j-th order correlation ($\langle v_\delta^j\rangle$, $\langle \delta v_\delta^{j-1}\rangle$ and $\langle \delta\delta v_\delta^{j-2}\rangle$) to $j \to \infty$ (Eq. A7). These terms are the consequence of nonlinear and non-Gaussian evolution, so we expect them to become non-negligible only in nonlinear regime and may become dominant in deeply nonlinear regime. However, since $\tilde{W} \to 0$ in deeply nonlinear regime, their contributions to $P^s_{\delta\delta}$ are significantly suppressed. For the same reason, $C_{NG,j+1}$ is suppressed by a factor $\sim \tilde{W}$, with respect to $C_{NG,j}$. Hence we propose to keep only the $j = 3$ term and neglect higher order corrections.

Fourier transforming $C_{NG,3}(\mathbf{r}, k_z)$ (Eq. A7), we obtain

$$\begin{aligned} C_{NG,3}(k,u) \ &= \ 2\int \frac{d^3\mathbf{k}_1}{(2\pi)^3} B_3(\mathbf{k}_1,\mathbf{k}_2,\mathbf{k}) \frac{k_{1z}k_z}{k_1^2} W(k_1) \\ &\times \left[\frac{k_z^2}{k^2}W(k) + \frac{k_zk_{2z}}{k_2^2}W(k_2) - 1\right] . \end{aligned} \quad (30)$$

Here, $\mathbf{k}_2 = -\mathbf{k}_1 - \mathbf{k}$. $B_3(\mathbf{k}_1,\mathbf{k}_2,\mathbf{k}_3)$ is the real space matter bispectrum. We notice that the ensemble average of $B_3(\mathbf{k}_1,\mathbf{k}_2,\mathbf{k}_3)$ is directly available from the same redshift surveys used for RSD measurement. Since $\sum_i \mathbf{k}_i = 0$, $\mathbf{k}_1$, $\mathbf{k}_2$ and $\mathbf{k}_3$ lie in the same plane. Due to the isotropy of the universe, $B_3(\mathbf{k}_1,\mathbf{k}_2,\mathbf{k}_3)$ does not depend on the inclination of the plane. So its value is equal to the case where all $\mathbf{k}$ lie in the plane perpendicular to the line of sight (namely the x-y plane). Redshift distortion does not alter the $k_z = 0$ Fourier mode. Namely, $\delta^s(\mathbf{k}_\perp, k_z = 0) = \delta(\mathbf{k}_\perp, k_z = 0)$. This means that B_3 can be directly measured from the observed Fourier mode with $k_{i,z} = 0$. Hence including $C_{NG,3}$ in the calculation does not introduce extra fitting parameters and hence does not weaken the cosmological constraints.

The same trick does not apply to $C_{NG,j\geq 4}$. They involve 4-th or higher order correlation $\langle \delta(\mathbf{k}_1), \cdots, \delta(\mathbf{k}_j)\rangle$, with $\mathbf{k}_1 + \cdots + \mathbf{k}_j = 0$. In general, $\mathbf{k}_i (i = 1,2,3,4\cdots,j)$ do not lie in the same plane. We are no longer able to infer their values from the $k_z = 0$ modes. However, due to extra suppression caused by $\tilde{W} < 1$, we do not expect these terms to be important. Nevertheless, the accuracy of neglecting these higher order terms must be quantified through N-body simulations.

D. A new formula on the redshift space power spectrum

We then propose the following formula for the redshift space power spectrum,

$$\begin{aligned} P^s(k,u) \ &\simeq \ \left\{P_{\delta\delta}(k)\left(1 + f\tilde{W}(k)u^2\right)^2\right. \quad (31) \\ &\left. + u^4 P_{\theta_S\theta_S}(k) + C_G(k,u) + C_{NG,3}(k,u)\right\} \\ &\times \ D_\delta^{\rm FOG}(ku) D_S^{\rm FOG}(ku) \exp\left[-\frac{k^2u^2\sigma_{v_B}^2}{H^2}\right] . \end{aligned}$$

In Eq. 31, $W(k) \equiv f\tilde{W}(k)$ and $P_{\theta_S\theta_S}(k)$ are the cosmological information we seek for. We address one more time that, *C_G and $C_{NG,3}$ are not free functions. They are uniquely determined by W.* This valuable property is achieved by the proposed velocity decomposition and, in particular, by the deterministic relation $\theta_\delta = \delta W$.

There are only very limited degrees of freedom in the FOG terms. Through Eq. 23, $D_\delta^{\rm FOG}(ku)$ and $D_S^{\rm FOG}(ku)$ may be well described by σ_{v_δ}, K_{4,v_δ}, σ_{v_S}, K_{4,v_S} and/or K_{6,v_δ}, K_{6,v_S}. Among them, σ_{v_δ} is determined by W (Eq. 27) and σ_{v_S} is determined by $P_{\theta_S\theta_S}$. So in principle they are not free parameters. Furthermore, since $\sigma^2_{v_B} \lesssim 100\sigma^2_{v_\delta}$ [70], we may be able to set $\sigma_{v_B} = 0$, depending on the desired accuracy.

1. Comparing to existing models

Here we compare the proposed RSD formula (Eq. 31) with a few existing RSD formulae. We choose these formulae because they can be compared with ours relatively straightforwardly. So this comparison is by no means complete. For brevity, we focus on the matter power spectrum for which we do not need to worry about the galaxy bias, especially the nonlinear/non-deterministic bias. (1) The Kaiser formula plus the FOG effect (hereafter KF),

$$P^s_{\delta\delta}(k,u) \simeq P_{\delta\delta}(k)(1 + fu^2)^2 D^{\rm FOG}(ku) \ . \quad (32)$$

This is perhaps the most commonly used RSD formula. (2) The Desjacques & Sheth 2010 formula (hereafter SD10, [47]),

$$\begin{aligned} P^s_{\delta\delta}(k,u) \ &= \ P_{\delta\delta}(k)(1 + fu^2)^2 \\ &\times \exp(-k_z^2\sigma_v^2/H^2) V_{\rm vir}(k_z) \ . \end{aligned} \quad (33)$$

Here, $V_{\rm vir}$ is the damping caused by random motions of virialized particles in halos. σ_v is the velocity dispersion of bulk motion. It improves over the KF formula by correctly recognizing the two velocity components (bulk motion and random motion). (3) The Scoccimarro 2004 formula (hereafter S04, [42]),

$$\begin{aligned} P^s_{\delta\delta}(k,u) \ &= \ \left(P_{\delta\delta}(k) + 2u^2P_{\delta\theta}(k) + u^4P_{\theta\theta}(k)\right) \\ &\times \exp(-k_z^2\sigma_v^2/H^2) \ . \end{aligned} \quad (34)$$

Here, σ_v can be treated as the one calculated from the perturbation theory or as a free parameter. It improves over KF by taking into account differences in the density and velocity nonlinear evolution. As a consequence, it does not assume a deterministic relation between density and velocity. (4) The Taruya et al. 2010 formula (hereafter T10, [53]),

$$\begin{aligned} P^s_{\delta\delta}(k,u) &= \big(P_{\delta\delta}(k) + 2u^2 P_{\delta\theta}(k) + u^4 P_{\theta\theta}(k) \\ &+ A(k,u) + B(k,u)\big) \exp(-k^2u^2\sigma_v^2/H^2) \ . \end{aligned} \quad (35)$$

The extra term A involves integral over the bispectrum. The term B involves convolution of two power spectra.

Comparing to Eq. 31, we recognize a number of corrections to existing formulae. Here we briefly summarize the most significant ones. (1) Both KF and DS10 fail to capture the $\tilde{W}$ correction on f. So f based on KF and DS10 is underestimated by a factor $\tilde{W}$. (2) S04 and T10 improve over KF and DS10 by correctly capturing the $\tilde{W}$ correction, although S04 and T10 do not make this correction explicitly. T10 further improves over S04 by including next order corrections (A and B). In the appendix B, we prove that $A = C_{NG,3}$ in the limit $\mathbf{v}_S \to 0$. However, T10 adopted the approximation $\epsilon_\delta = 0$ (equivalently $\langle v_1 v_2\rangle = 0$). so it fails to capture some terms of the same order as A and B, as we do (Eq. A6). More importantly, calculating A and B requires heavy modeling or simulation calibration. Our Eq. 31 avoids these uncertainties. (3) The FOG effect is caused by three distinctly different velocity components, so it may not follow a simple function form. For this point, the closest match to our formula is DS10. These complexities can bias the interpretation of the inferred σ_v from RSD.

E. Implications on the RSD cosmology

Our analysis above shows that what one can infer from RSD is the combination $f\tilde{W}(k)$ instead of f. Since $\tilde{W}(k) \sim 0.9$ at $k = 0.1h/\mathrm{Mpc}$ and $z = 0$, this can cause 10% underestimation in f. We expect that it is at least a significant source causing the recently found underestimation in f [63–68]. This systematical error overwhelms the 1% level statistical accuracy in f by stage IV dark energy projects. Our work provides a promising way to overcome this severe systematical error. To do so we need to robustly model $\tilde{W}$, with the help of analytical and numerical tools.

The $\tilde{W}$ correction affects many applications of redshift distortion. For example, [25] proposed an E_G estimator combining weak lensing and redshift distortion to test general relativity at cosmological scale. This estimator is insensitive to galaxy bias and is also less affected by initial fluctuations. [28] made the first E_G measurement and found $E_G = 0.39 \pm 0.06$ at an effective redshift 0.32 and $O(10)\mathrm{Mpc}/h$ scale. This measurement confirms general relativity within $\sim 20\%$ observational uncertainties. This result has been used to perform consistency tests of the ΛCDM cosmology and confirmed its validity [78]. Given the existence of $\tilde{W} \neq 1$, the expectation value of E_G should be corrected by a factor $1/\tilde{W}$,

$$E_G = \left[\frac{G_{\rm eff}}{G_N}\frac{\Omega_0}{f}\right]\frac{1}{\tilde{W}(k)} \ . \quad (36)$$

Future experiments such as BigBOSS+LSST, BigBOSS+Planck CMB lensing, Euclid or other combinations of spectroscopic surveys and imaging surveys are capable of measuring E_G to 1% level statistical accuracy [25]. For these measurements, The $1/\tilde{W}$ correction is needed in order to correctly interpret the measured E_G.

F. To do list

Most statistics discussed in this section are too complicated to evaluate analytically. In companion papers [1], we will use N-body simulations to numerically evaluate these statistics. An incomplete investigation list includes

- The damping function $D^{\rm FOG}_\delta(ku)$, $D^{\rm FOG}_S(ku)$ and $D^{\rm FOG}_B(ku)$. In particular, we will investigate the usage of the cumulant expansion theorem (Eq. 23). We will check if including K_4 and/or K_6 describes $D^{\rm FOG}_\delta(ku)$ and $D^{\rm FOG}_S(ku)$ accurately at scales of interest. We will also check the accuracy of Eq. 24.
- ϵ_δ, ϵ_S and ϵ_B. In particular, we will quantify the accuracy of Eq. 21 & 25.
- The accuracy of the proposed RSD formula (Eq. 31). We will measure $C_{G,j}$ and $C_{NG,j}$ from simulations. We will also quantify the relative contribution of the leading terms, namely $C_{G,4}$ to C_G, $C_{NG,3}$ to C_{NG} and $P_{\theta_S\theta_S}$ with respect to C_S. We will seek the possibility to further improve the RSD modeling, if needed.

IV. RECONSTRUCTION OF THE 3D VELOCITY FIELD IN REDSHIFT SURVEYS

So far we focus on inferring the statistical average of the velocity field including $W \propto P_{\delta\theta}$, $P_{v_Sv_S}$, σ_{v_δ}, σ_{v_S} and σ_{v_B}. Can we go a step further to construct the full 3D velocity field? The gain would be huge since the 3D velocity field contains much more information and has much more applications. One of such applications is to search for the missing baryons through the diffuse kinetic Sunyaev Zel'dovich (kSZ) effect [79] caused by the intergalactic medium. However, although the ACT collaboration has reported the first detection of the kSZ effect of galaxy clusters [80], the diffuse kSZ is still elusive even to the state of art surveys such as ACT [80, 81] and SPT [82, 83], due to various overwhelming contaminations. The measurement can be revolutionized by the kinetic SZ tomography [84, 85]. The key is to reconstruct the galaxy velocity field. One can then construct the galaxy momentum field. It can then be correlated with CMB to measure the kSZ effect while automatically eliminating all contaminations of scalar type. A combination of BigBOSS and Planck is promising to measure kSZ to better than 10σ at a number of redshift bins [85].

How to reconstruct the 3D velocity field? If we can, which velocity component can be reconstructed? There are numerous works over a long history. We are not at a stage to overview these works. Rather, we outline our approach, based upon the proposed velocity decomposition.

Since observationally we only have the density field, which is a scalar field, the information budget does not allow us to reconstruct all the three $\mathbf{v}_\delta$, $\mathbf{v}_S$ and $\mathbf{v}_B$ vector fields. However, since $\mathbf{v}_\delta$ is completely correlated with the density field, it is promising to reconstruct $\mathbf{v}_\delta$ from the observed density field. Eq. 3 guides us to propose a linear estimator for the 3D peculiar velocity reconstruction through the 3D density field. Since we observe the redshift space overdensity δ^s instead, this linear estimator should operate on $\delta^s(\mathbf{k})$,

$$\hat{\theta}_\delta(\mathbf{k})=\delta^s(\mathbf{k})\hat{W}^s(\mathbf{k}) \ . \tag{37}$$

We use the superscript "s" to denote properties in redshift space. $\hat{W}^s$ corresponds to an anisotropic window function operating on the anistropic density field in redshift space. Now the reconstruction of the stochastic 3D velocity filed is simplified into th reconstruction of a deterministic function W^s. Due to the axial symmetry along the light of sight, $W^s(\mathbf{k})=W^s(k,u)$. So it only has 2D degrees of freedom. These degrees of freedom are further limited by the asymptotic behaviors of $W^s(k,u)$ at $ku\rightarrow 0$ and at $k\rightarrow\infty$.

We want the peculiar velocity estimator (Eq. 37) to have no multiplicative error. This requires

$$\hat{W}^s(\mathbf{k})=\frac{W(k)}{C_v(\mathbf{k})}=\frac{W(k)}{r^{rs}(\mathbf{k})}\sqrt{\frac{P_{\delta\delta}(k)}{P^s_{\delta\delta}(\mathbf{k})}} \ . \tag{38}$$

W^s differs from the real space one by a direction dependent factor $1/C_v(\mathbf{k})$. This factors arises because the redshift space density δ^s is not completely correlated with the real space density δ. To better understand this point and to derive Eq. 38, we carry out a decomposition of δ^s into two parts,

$$\delta^s=\delta^s_v+\delta^s_S \ . \tag{39}$$

We require δ^s_v to be completely correlated with the underlying overdensity δ and hence to θ_δ. This is the part that we can use to recover the peculiar velocity. For this reason, we label this part with a subscript "v". δ^s_S is uncorrelated with δ and θ_δ. It causes the stochasticity in δ-δ^s relation and contaminates the velocity reconstruction. So it is labelled with a subscript "S". Since δ_v is completely correlated with δ,

$$\delta^s_v(\mathbf{k})=\delta(\mathbf{k})C_v(\mathbf{k}) \ , \tag{40}$$

with the deterministic function C_v to be determined. Through the relation $\langle\delta(\mathbf{k})\delta^s(\mathbf{k}^{'})\rangle=\langle\delta(\mathbf{k})\delta^s_v(\mathbf{k}^{'})\rangle=\langle\delta(\mathbf{k})\delta(\mathbf{k}^{'})\rangle C_v(\mathbf{k})$, we obtain

$$C_v(\mathbf{k})=\frac{P^{rs}_{\delta\delta}(\mathbf{k})}{P_{\delta\delta}(k)}=r^{rs}(\mathbf{k})\sqrt{\frac{P^s_{\delta\delta}(k,u)}{P_{\delta\delta}(k)}} \ . \tag{41}$$

Here, $P^{rs}_{\delta\delta}$ is the cross power spectrum between δ and δ^s. $r^{rs}_{\delta\delta}$ is the corresponding cross correlation coefficient. It has the asymptotic behavior $r^{rs}\rightarrow 1$ when $ku\rightarrow 0$ and $r^{rs}\rightarrow 0$ when $ku\rightarrow\infty$. Notice that r^{rs} depends on both k and u. So do C_v and W^s. Hereafter we will write them as $r^{rs}(k,u)$, $W^s(k,u)$ and $C_v(k,u)$ to highlight these dependences.

Both $P_{\delta\delta}(k)$ and $P^s_{\delta\delta}(k,u)$ are observables. To evaluate $\hat{W}^s$ requires just one extra input, $r^{rs}(k,u)$. r^{rs} has a well defined asymptotic behavior $r^{rs}\rightarrow 1$ when $ku\rightarrow 0$ and $r^{rs}\rightarrow 0$ when $|ku|\rightarrow\infty$. In the appendix C, we show that r^{rs} is uniquely fixed by W and other quantities which can be inferred from $P^s_{\delta\delta}(k,u)$. Hence the observed RSD allows us to figure out W^s and then carry out the velocity reconstruction. In this sense, *RSD is a source of information crucial for the velocity reconstruction, instead of source of noise as in many other apprroaches of velocity reconstruction.*

In the appendix D, we propose another approach to reconstruct the 3D velocity field. It shows more clearly the crucial role of RSD in the velocity reconstruction.

A. Errors int the reconstruction and remodies

A correct $W^s(k,u)$ allows to reconstruct $\mathbf{v}_\delta$ free of multiplicative error. Unfortunately, additive errors persist, due to the stochastic component δ^s_S. The reconstructed velocity divergence is

$$\begin{aligned}\hat{\theta}_\delta(\mathbf{k}) &= \theta_\delta(\mathbf{k})+\theta^s_S(\mathbf{k}) \ , \\ \theta^s_S(\mathbf{k}) &\equiv \delta^s_S(\mathbf{k})\hat{W}^s(k,u) \ .\end{aligned} \tag{42}$$

The additive error $v^s_S(\mathbf{k})=iH\theta^s_S(\mathbf{k})\mathbf{k}/k^2$ induces an additive error to the auto power spectrum directly measured from $\hat{\theta}_\delta$. So cosmological applications of the directly measured auto power spectrum can be very limited, if any.

However, a good thing is that its cross power spectrum with the density distribution is still unbiased,

$$\hat{P}_{\delta\theta}=P_{\delta\theta}=P_{\delta\theta_\delta} \ . \tag{43}$$

For the same reason, the additive error does not bias the kSZ tomography [84, 85] and hence does not bias the effort to search for missing baryons.

Since θ_δ is completely correlated with the matter density, we can measure the auto power spectrum unbiasedly, through the relation

$$P_{\theta_\delta\theta_\delta}=\frac{P^2_{\delta\theta_\delta}}{P_{\delta\delta}} \ . \tag{44}$$

B. To do list

Through N-body simulations, a number of key issues will be investigated in future works,

- $r^{rs}(k,u)$, $W^s(k,u)$ and $C_v(k,u)$. We are then able to quantify the additive error in the reconstructed velocity. Furthermore, we want to understand the origin of δ^s_S, which causes the stochasticity in the δ-δ^s relation and degrades the reconstruction performance.

- The accuracy of Eq. C6 to model r^{rs}.

- The accuracy of the velocity reconstruction. It is determined by the accuracy of the inferred W from the observed RSD and the accuracy of the modeled r^{rs}. Measurement errors in the galaxy distribution such as shot noise further complicates the reconstruction. We will take them into account for more realistic quantification of the reconstruction performance.

- Further investigation of the velocity reconstruction approach proposed in the appendix D.

V. FROM MATTER DISTRIBUTION TO GALAXY DISTRIBUTION

In reality, we have 3D galaxy distribution instead of 3D matter distribution. The above methods to model the matter redshift space distortion and to carry out velocity reconstruction can be extended to the 3D galaxy distribution straightforwardly and robustly. To do so, we need to decompose the irrotational galaxy velocity $\mathbf{v}_E$ into two eigen-modes such that one part is completely correlated with the galaxy overdensity and the other part is completely uncorrelated. We can then replace quantities of the matter field in previous sections to that of the corresponding galaxy field. For example, W should be interpretted as $W = P_{g\theta}/P_{gg}$ where the subscript "g" denotes properties of galaxies. Now $W = \beta\tilde{W}$ and $\beta = f/b_g(k \rightarrow 0)$. In fact, we can replace the subscript "δ" in previous sections with the subscript "g" to obtain results applicable to galaxies.

Nevertheless, there is an important exception. The $\tilde{W}$ in the E_G estimator (Eq. 36) should be still interpreted as that of the matter field instead of the galaxy field. By the construction, $E_G \propto P_{g\delta}/P_{g\theta}$ [25]. Here, δ is the matter overdensity. We can decompose the galaxy velocity with respect to the matter field, instead of the galaxy number density field. Under reasonable assumptions of $P_{g\theta_S} = 0$ [86] and no galaxy velocity bias at relevant scales, $P_{g\delta}/P_{g\theta} = P_{g\delta}/(WP_{g\delta}) \propto 1/(f\tilde{W})$. This property is desirable since the correction term $\tilde{W}$ can be robustly quantified through N-body simulations, free of uncertainties in modeling galaxy formation.

This straightforward extension to the galaxy field further demonstrates the power of our approach. For example, it significantly alleviates the problem of galaxy bias in the velocity reconstruction. Even better, in the limit of a deterministic bias ($\delta_g = b_g\delta$), completely overcome it. Now $W = P_{g\theta}/P_{gg} \propto 1/b_g$. The reconstructed 3D velocity is $\propto W\delta_g \propto b_g^0$, independent of b_g. This is also the case for the inferred velocity power spectrum $P_{\theta_g\theta_g} = P^2_{g\theta_g}/P_{gg}$.

In future works we will redo the analysis of the matter density field for the halo number density. We will then proceed to mock catalogs of galaxies. Eventually we plan to develop efficient codes applicable to real data of spectroscopic redshift surveys.

VI. DISCUSSIONS AND SUMMARY

We have laid out the methodology to carry out 3D velocity reconstruction from 3D matter and galaxy distribution. The method is based upon a velocity decomposition into three eigen-modes with physical motivation and of mathematical uniqueness. The same decomposition also helps the RSD modeling and we have derived a new RSD formula. Through it we find that the inferred structure growth rate based upon some simplified versions of RSD modeling can be severely underestimated. In a series of companion papers [1] we will analyze N-body simulations to measure statistics of the three velocity eigen-modes, to test the accuracy of the proposed RSD formula and to quantify the performance of the proposed velocity reconstruction.

Acknowledgments

This work was supported by the national science foundation of China (grant No. 11025316 & 11121062 and 10873035 & 11133003), National Basic Research Program of China (973 Program) under grant No.2009CB24901 and the CAS/SAFEA International Partnership Program for Creative Research Teams (KJCX2-YW-T23).

Appendix A: Calculating the $\mathbf{v}_\delta$ induced RSD

Throughout this section we only deal with the velocity component $\mathbf{v}_\delta$. Hence for brevity we neglect the subscript "δ" and denote $v_{1z,\delta} = v_1$, $v_{2z,\delta} = v_2$, $\lambda_{1,2} \equiv ik_z v_{1,2}/H$ and $\lambda_\delta \equiv \lambda_1 - \lambda_2$. We will adopt two tricks in [42, 53] to faciliate the derivation. The first is the relation $\langle \delta_1 \exp \lambda_\delta \rangle = \frac{\partial}{\partial a_1}\langle \exp(\lambda_\delta + a_1\delta_1)\rangle_{a_1=0}$. In combination with the cumulant expansion theorem $\langle \exp X \rangle = \exp(\sum \langle X^n \rangle_c/n!)$, we have

$$\langle \delta_1 \exp \lambda_\delta \rangle \;=\; \langle \exp \lambda_\delta \rangle \sum_{n\geq 1} \frac{n\langle \lambda_\delta^{n-1}\delta_1\rangle_c}{n!}$$

$$= \langle \exp\lambda_\delta\rangle \sum_{n\geq 0} \frac{\langle \lambda_\delta^n \delta_1\rangle_c}{n!} \ . \tag{A1}$$

The second relation is $\langle \delta_1\delta_2 \exp\lambda_\delta\rangle = \frac{\partial^2}{\partial a_1 \partial a_2}\langle \exp(\lambda_\delta + a_1\delta_1 + a_2\delta_2)\rangle_{a_1=0,a_2=0}$. Again with the cumulant expansion theorem, we have

$$\langle \delta_1\delta_2 \exp\lambda_\delta\rangle = \langle \exp\lambda_\delta\rangle \times \left[\sum_{j\geq 1}\frac{\langle \lambda_\delta^j\delta_1\rangle_c}{j!}\sum_{n\geq 1}\frac{\langle \lambda^n\delta_2\rangle_c}{n!} + \sum_{n\geq 0}\frac{\langle \delta_1\delta_2\lambda_\delta^n\rangle_c}{n!}\right] \ . \tag{A2}$$

Putting all pieces together, we obtain

$$\begin{aligned}\langle (1+\delta_1)(1+\delta_2)\exp\lambda_\delta\rangle &= D_\delta^{\rm FOG}(k_z)(1+\epsilon_\delta(\mathbf{r},k_z)) \\ &\left(1+\sum_{n\geq 1}\frac{\langle \lambda_\delta^n(\delta_1+\delta_2)\rangle_c}{n!} + \sum_{n\geq 0}\frac{\langle \delta_1\delta_2\lambda_\delta^n\rangle_c}{n!}\right. \\ &\left. + \sum_{j\geq 1}\frac{\langle \lambda_\delta^j\delta_1\rangle_c}{j!}\sum_{n\geq 1}\frac{\langle \lambda_\delta^n\delta_2\rangle_c}{n!}\right) \ .\end{aligned} \tag{A3}$$

Through the cumulant expansion theorem, we have

$$\begin{aligned}1+\epsilon_\delta(\mathbf{r},k_z) &= \exp\left[\sum_{\alpha+\beta\geq 2}\frac{\langle \lambda_\delta^{\alpha+\beta}\rangle_c}{(\alpha+\beta)!} - \frac{\langle \lambda_1^\alpha\rangle_c}{\alpha!}\frac{\langle -\lambda_2^\beta\rangle_c}{\beta!}\right] \\ &= \exp\left[\frac{k_z^2\langle v_1v_2\rangle}{H^2} + O(v^4)\right] \ .\end{aligned}$$

Terms odd in the power of v vanish due to symmetry reason. For example, due to symmetry of $v \leftrightarrow -v$, we have $\langle (v_1-v_2)^3\rangle = 0$, $\langle v_1^3\rangle = \langle v_2^3\rangle$. So $\langle v_1v_2^2\rangle - \langle v_1^2v_2\rangle = 0$. Terms of $O(v^3)$ do not show in Eq. A4. Expression including terms of order v^4 can be obtained following Eq. 25.

Collecting tersm of the same orders together, we have

$$\begin{aligned}\langle (1+\delta_1)(1+\delta_2)\exp\lambda_\delta\rangle &= D_\delta^{\rm FOG}(k_z) \\ \times\left[1+\langle \delta_1\delta_2\rangle + i\frac{k_z}{H}\langle \delta_2v_1-\delta_1v_2\rangle + \frac{k_z^2}{H^2}\langle v_1v_2\rangle\right. & \\ \left. + C_{NG}(\mathbf{r},k_z) + C_G(\mathbf{r},k_z)\right] \ . &\end{aligned} \tag{A4}$$

Two correction terms C_G and C_{NG} show up. C_G includes all high order corrections, if the density and velocity fields are Gaussian. It solely arises from the nonlinear real space-redshift space mapping. So we denote it with a subscript "G". It has an exact analytical expression,

$$\begin{aligned}C_G(\mathbf{r},k_z) &= \left[\exp(k_z^2\langle v_1v_2\rangle/H^2)-1\right] \\ &\times \left(\langle \delta_1\delta_2\rangle + i\frac{k_z}{H}\langle \delta_2v_1-\delta_1v_2\rangle\right) \\ &+ \frac{k_z^2}{H^2}\langle \delta_1v_2\rangle\langle \delta_2v_1\rangle\exp(k_z^2\langle v_1v_2\rangle/H^2) \\ &+ \left[\exp(k_z^2\langle v_1v_2\rangle/H^2) - \frac{k_z^2}{H^2}\langle v_1v_2\rangle\right] \ .\end{aligned} \tag{A5}$$

We notice that this analytical result for Gaussian field has been derived by [42] and shown as their Eq. 32.

As shown in §III, C_G can be robustly calculated combining observations without knowing the underlying cosmology and without introducing extra unknown parameters. The leading order term is 4-th power in the density field, with

$$\begin{aligned}C_{G,4}(\mathbf{r},k_z) &= \frac{k_z^2\langle v_1v_2\rangle}{H^2}\left(\langle \delta_1\delta_2\rangle + i\frac{k_z}{H}\langle (v_1-v_2)(\delta_1+\delta_2)\rangle\right) \\ &+ \frac{k_z^2}{H^2}\langle \delta_1v_2\rangle\langle \delta_2v_1\rangle + \frac{1}{2}\frac{k_z^4}{H^4}\langle v_1v_2\rangle^2 \ .\end{aligned} \tag{A6}$$

To the opposite, C_{NG} solely arises from non-Gaussianities. For this reason, we denote it with the subscript "NG". It is the sum of an infinite series of j-th order correlations with $j\geq 3$.

$$\begin{aligned}C_{NG} &= \sum_{j\geq 3} C_{NG,j}(\mathbf{r},k_z) \\ &= \left[i\frac{k_z\langle \delta_1\delta_2(v_1-v_2)\rangle_c}{H} - \frac{k_z^2\langle (v_1-v_2)^2(\delta_1+\delta_2)\rangle_c}{2H^2}\right] \\ &+\cdots \ .\end{aligned} \tag{A7}$$

In the above equation, we only show the explicit expression of $C_{NG,j=3}$. It is valid even if higher order velocity correlation terms are included in ϵ_δ (Eq. A4).

So far the results are exact. To proceed, we have to make reasonable approximation on C_{NG}. We argue that, due to extra suppression $\tilde{W} \ll 1$ in the deeply nonlinear region, higher order non-Gaussian terms are expected to be smaller than $C_{NG,j=3}$. So keeping only $C_{NG,j=3}$ should be reasonably accurate. Nevertheless, we will check this approximation in the future, through N-body simulations. If needed, $C_{NG,j\geq 4}$ may be included in the calculation.

In the appendix B, we will prove that $C_{NG,j=3}$ is equivalent to the term A in [53]. Strictly speaking, its Fourier transform $C_{NG,j=3}(k,u) = A(k,u)$ in the limit that $\mathbf{v}_S \to 0$.

Appendix B: The $C_{NG,3}$-A relation

The term A is derived by [53] as an additive correction to the Kaiser formula. [53] does not distinguish between $\mathbf{v}_\delta$ and $\mathbf{v}_S$, so the velocity showing up in the expression of A is $\mathbf{v}_E = \mathbf{v}_\delta + \mathbf{v}_S$. We consider the limit $\mathbf{v}_S = 0$. Re-expressed in our notations, A in [53] is

$$\begin{aligned}A(k,u) &= i\frac{k_z}{H}\int\langle (v_1-v_2)(\delta_1-\frac{\nabla_1v_1}{H})(\delta_2-\frac{\nabla_2v_2}{H})\rangle \\ &\quad \exp(-i\mathbf{k}\cdot\mathbf{r})d^3\mathbf{r} \qquad \text{(B1)} \\ &= ik_z\int\langle (v_1-v_2)\delta_1\delta_2\rangle\exp(-i\mathbf{k}\cdot(\mathbf{r})d^3\mathbf{r} \\ &+ i\frac{k_z}{H^2}\int\langle (v_2\delta_2\nabla_1v_1 - v_1\delta_1\nabla_2v_2 + \delta_1v_2\nabla_2v_2\end{aligned}$$

$$-\delta_2 v_1 \nabla_1 v_1)\rangle \exp(i\mathbf{k}\cdot(\mathbf{x}_1-\mathbf{x}_2))d^3\mathbf{x}_1 d^3\mathbf{x}_2 \frac{1}{V}$$
$$+\ i\frac{k_z}{H^3}\langle (v_1-v_2)\nabla_1 v_1 \nabla_2 v_2\rangle$$
$$\exp(i\mathbf{k}\cdot(\mathbf{x}_1-\mathbf{x}_2))d^3\mathbf{x}_1 d^3\mathbf{x}_2 \frac{1}{V}\ .$$

Here V is the total volume. Since $v_2\delta_2\nabla_1 v_1 \exp(i\mathbf{k}\cdot\mathbf{x}_1) = \nabla_1[v_2\delta_2 v_1 \exp(i\mathbf{k}\cdot\mathbf{x}_1)] - ik_z v_2\delta_2 v_1 \exp(i\mathbf{k}\cdot\mathbf{x}_1)$ and since $\nabla_1(\cdots)$ integrates to be zero, the term $v_2\delta_2\nabla_1 v_1$ in the above equation can be replaced by the term $-ik_z v_2\delta_2 v_1$. In total we can do the following replacements in Eq. B1,

$$\begin{aligned}
v_2\delta_2\nabla_1 v_1 &\rightarrow -ik_z v_2\delta_2 v_1\ , \\
v_1\delta_1\nabla_2 v_2 &\rightarrow ik_z v_1\delta_1 v_2\ , \\
\delta_1 v_2\nabla_2 v_2 &\rightarrow ik_z\frac{1}{2}\delta_1 v_2^2\ , \\
\delta_2 v_1\nabla_1 v_1 &\rightarrow -ik_z\frac{1}{2}\delta_2 v_1^2\ , \\
v_1\nabla_1 v_1\nabla_2 v_2 &\rightarrow k_z^2\frac{1}{2}v_1^2 v_2\ , \\
v_2\nabla_1 v_1\nabla_2 v_2 &\rightarrow k_z^2\frac{1}{2}v_2^2 v_1 \qquad \text{(B2)}
\end{aligned}$$

Comparing to Eq. A6, we prove that, in the limit $\mathbf{v}_S\rightarrow 0$, $C_{NG,3}(k,u) = A(k,u)$.

On the other hand, our $C_{G,4}$ is not equal to the B term in [53], due to differences in the methods and differences in approximations made. For example, [53] sets $\epsilon_\delta = 0$ in their Eq. 18. Inclusion of $\epsilon_\delta \neq 0$ in our derivation brings up new terms such as the term $\langle v_1 v_2\rangle^2$ in Eq. A7. In future works we will test against N-body simulations to compare the two results.

Appendix C: Modeling $r^{rs}(k,u)$

Following the derivation of $P^s_{\delta\delta}$, the real space -redshift space density cross power spectrum $P^{rs}_{\delta\delta}$ is given by

$$\begin{aligned}
P^{rs}_{\delta\delta}(k,u) &= \int \langle (1+\delta_1)(1+\delta_2)\exp[ik_z v_{1z}/H]\rangle \qquad \text{(C1)} \\
&\quad \exp(-i\mathbf{k}\cdot\mathbf{r})d^3\mathbf{r} \\
&= \int \left\langle (1+\delta_1)(1+\delta_2)\exp\left(i\frac{k_z v_{1\delta,z}}{H}\right)\right\rangle \\
&\quad \exp(-i\mathbf{k}\cdot\mathbf{r})d^3\mathbf{r}\sqrt{D_S^{\rm FOG}(k_z)D_B^{\rm FOG}(k_z)}\ .
\end{aligned}$$

Replacing λ_δ in Eq. A3 with λ_1, we obtain

$$\begin{aligned}
&\langle (1+\delta_1)(1+\delta_2)\exp\lambda_1\rangle = \langle \exp\lambda_1\rangle \\
&\left(1+\sum_{n\geq 1}\frac{\langle \lambda_1^n(\delta_1+\delta_2)\rangle_c}{n!}+\sum_{n\geq 0}\frac{\langle \delta_1\delta_2\lambda_1^n\rangle_c}{n!}\right. \qquad \text{(C2)} \\
&\left. +\sum_{j\geq 1}\frac{\langle \lambda_1^j\delta_1\rangle_c}{j!}\sum_{n\geq 1}\frac{\langle \lambda_1^n\delta_2\rangle_c}{n!}\right)\ .
\end{aligned}$$

We then have

$$\begin{aligned}
P^{rs}_{\delta\delta}(k,u) &= \left[P_{\delta\delta}(k)(1+f\tilde{W}(k)u^2)+C^{rs}_{NG}(k,u)\right] \qquad \text{(C3)} \\
&\quad \times\sqrt{D_\delta^{\rm FOG}(k_z)D_S^{\rm FOG}(k_z)D_B^{\rm FOG}(ku)}\ .
\end{aligned}$$

The high order correction term

$$\begin{aligned}
C^{rs}_{NG}(k,u) &= y\times P_{\delta\delta}(k)f\tilde{W}u^2+\int \exp(-i\mathbf{k}\cdot\mathbf{r})d^3\mathbf{r} \qquad \text{(C4)} \\
&\quad \times\left[\sum_{n\geq 1}\frac{\langle \delta_1\delta_2\lambda_1^n\rangle_c}{n!}+\sum_{n\geq 2}\frac{\langle \lambda_1^n\delta_2\rangle_c}{n!}(1+y)\right]\ .
\end{aligned}$$

Here, $y \equiv \sum_{j\geq 1}\langle \lambda_1^j\delta_1\rangle_c/j! = \sum_{j\geq 2}\langle \lambda_1^j\delta_1\rangle_c/j!$. We can resum C^{rs}_{NG} in order of the power of δ,

$$\begin{aligned}
C^{rs}_{NG}(k,u) &= \sum_{j\geq 3} C^{rs}_{NG,j}(k,u) \qquad \text{(C5)} \\
&= \int e^{-i\mathbf{k}\cdot\mathbf{r}}d^3\mathbf{r}\left[\langle \delta_1\delta_2\lambda_1\rangle_c+\frac{\langle \lambda_1^2\delta_2\rangle_c}{2!}\right]+\cdots
\end{aligned}$$

The last expression only shows $C^{rs}_{NG,3}$. Finally we obtain the expression for r^{rs},

$$r^{rs}(k,u) \simeq \frac{1+\frac{C^{rs}_{NG,3}(k,u)}{P_{\delta\delta}(k)(1+f\tilde{W}(k)u^2)}}{\sqrt{1+\frac{P_{\theta_S\theta_S}(k)u^4+C_{NG,3}(k,u)+C_G(k,u)}{P_{\delta\delta}(k)(1+f\tilde{W}(k)u^2)^2}}}\ . \qquad \text{(C6)}$$

Evaluating r^{rs} requires $P_{\delta\delta}$, B_3, W and $P_{\theta_S\theta_S}$. The first two are observables, as discussed in §III. The last two can be inferred from the observed $P^s_{\delta\delta}$ (§III D). So there is no uncertainty involved in predicting r^{rs}. This will also be the case for the window function W^s (Eq. 38) required for velocity reconstruction.

Appendix D: An alternative approach to reconstruct the 3D velocity field

As shown in §IV, the key to reconstruction the 3D $\mathbf{v}_\delta$ is to infer the correct window function W^s. The approach discussed in §IV is straightforward. But it relies on the RSD modeling and is hence susceptible to inaccuracies therein. Here we propose an alternative to simultaneously estimate W^s and reconstruct $\mathbf{v}_\delta$. It avoids modeling the $\mathbf{v}_\delta$ induced RSD, the most difficult part in the RSD modeling. So it is less susceptible to uncertainties in the RSD modeling.

The guideline is that, if we construct W^s and $\mathbf{v}_\delta$ correctly, we can move particles/galaxies back to their real space positions. This will eliminate the $\mathbf{v}_\delta$ induced RSD and hence reduce anisotropies in the power spectrum after moving (hereafter we denote it as $P^s_{\rm move}(\mathbf{k})$). To further demonstrate this point, let us consider the limit of $\mathbf{v}_S = 0$, $\mathbf{v}_B = 0$, $\delta^s_S = 0$ and no measurement noise. Under this limit, a correct guess of W^s will faithfully recover $\mathbf{v}_\delta$. Moving the particles back to their real space positions using this $\mathbf{v}_\delta$, anisotropies in $P_{\rm move}(\mathbf{k})$ will be completely eliminated and we recover the isotropic real space power spectrum ($P_{\rm move}(\mathbf{k}) = P(k)$). This suggests that, by tuning W^s until the $P_{\rm move}(\mathbf{k})$ reaches isotropy, we can recover the correct W^s and hence recontruct the velocity correctly.

The real situation is more complicated, due to the fact that $\mathbf{v}_S \neq 0$, $\mathbf{v}_B \neq 0$, $\delta^s_S \neq 0$ and the existence of measurement noise such as shot noise in the galaxy number distribution. However, none of them is correlated with the real space density and none of them can cause anisotropic pattern the same as $\mathbf{v}_\delta$. The W^s reconstructs $\mathbf{v}_\delta$ without multiplicative error will cause

$$P_{\rm move}(k,u) = \int (1+\langle\delta_1\delta_2\rangle) D_{\rm move}(k_z,\mathbf{r}) e^{-i\mathbf{k}\cdot\mathbf{r}} d^3\mathbf{r} \ . \tag{D1}$$

Like P^s, $P_{\rm move}$ only depends on k and u. So we write these dependences explicitly. Here

$$D_{\rm move}(k_z,\mathbf{r}) \ \equiv \ \left\langle e^{\lambda_S+\lambda_B-ik_z(v^s_{1z,S}-v^s_{2z,S})/H}\right\rangle \ . \tag{D2}$$

We also define a $\epsilon_{\rm move}$ through

$$1+\epsilon_{\rm move}(k_z,\mathbf{r}) \equiv \frac{D_{\rm move}(k_z,\mathbf{r})}{D_{\rm move}(k_z, r\rightarrow\infty) = D^{\rm FOG}_{\rm move}(k_z)} \tag{D3}$$

Since $\mathbf{v}_B$ is uncorrelated with $\mathbf{v}_S$ and $\mathbf{v}^s_S$, we have $D^{\rm FOG}_{\rm move} = D^{\rm FOG}_B(k_z)\langle e^{ik_z\Delta v_S/H}\rangle^2$. Here, $\Delta v_S \equiv v_{z,S} - v^s_{z,S}$. So far we have neglected shot noise in the galaxy distribution. Since it does not correlate with other components, it only causes damping. This effect can be completely described by a damping function $D^{\rm FOG}_{\rm shot}(ku)$, the same as the case of $\mathbf{v}_B$. For brevity, we will not consider this measurement noise hereafter.

A more complicated issue to deal with is $\mathbf{v}^s_S$, arising from the stochastic component in the redshift space overdensity δ^s (Eq. 39). $\mathbf{v}_S$ and $\mathbf{v}^s_S$ are correlated, so we can not do the average $\langle e^{ik_z\Delta v_S/H}\rangle^2$ seperately for $v_{z,S}$ and $v^s_{z,S}$. To see their correlation, let us check the limit $k\rightarrow 0$. Now we have $\delta^s \simeq \delta - \nabla_z v_z/H$, the starting point to derive the Kaiser formula. Since $\delta_s = (\delta - \nabla_z v_{z,\delta}/H) - \nabla_z v_{z,S}/H$, we obtain $\delta^s_S \simeq -\nabla_z v_{z,S}/H$. Through the relation $\theta^s_S(\mathbf{k}) = \delta^s_S(\mathbf{k})W^s(\mathbf{k})$, we have $\mathbf{v}^s_S(\mathbf{k}) \simeq (\mathbf{v}_S(\mathbf{k})\cdot\hat{k})u^2W^s(\mathbf{k})\hat{k}$. Notice that *the velocity field $\mathbf{v}^s_S$ is statistically anisotropic*. Under this limit, $\mathbf{v}^s_S$ is completely correlated with $\mathbf{v}^s$. The $\mathbf{v}_S$-$\mathbf{v}^s_S$ relation beyond this limiting case is too complicated to discuss here. In future works we will use N-body simulations to quantify it.

Using the relation

$$1+\epsilon_{\rm move}(k_z,\mathbf{r}) = e^{k_z^2\langle\Delta v_{1S}\Delta v_{2S}\rangle/H^2+O(\Delta v_S^4)} \ , \tag{D4}$$

we obtain

$$\begin{aligned} P_{\rm move}(k,u) \ &= \ \left[P_{\delta\delta}(k) + P_{\Delta v\Delta v}(k,u)u^4 + \cdots\right] \\ &\quad \times D^{\rm FOG}_{\rm move}(k_z) \ . \end{aligned} \tag{D5}$$

Here, $P_{\Delta v\Delta v}(k,u)$ is the power spectrum of $\Delta\mathbf{v}_S \equiv \mathbf{v}_S - \mathbf{v}^s_S$. Due to the intrinsically anisotropic $\mathbf{v}^s_S$, $P_{\Delta v\Delta v}(\mathbf{k})$ is also anisotropic and depends on both k and u. At large scale limit,

$$\begin{aligned} P_{\Delta v\Delta v}(\mathbf{k}) \ &\simeq \ P_{\theta_S\theta_S}(k)(1-u^2W^s(\mathbf{k}))^2 \\ &\simeq \ P_{\theta_S\theta_S}(k)\frac{1}{(1+f\tilde{W}u^2)^2} \ . \end{aligned} \tag{D6}$$

The situation beyond this limit is too complicated to discuss in analytical ways here and will be postponed for future study. Nevertheless, $P_{\Delta v\Delta v}(\mathbf{k})$ has a generic property $P_{\Delta v\Delta v}(k,u)/P_{\delta\delta}(k)\rightarrow 0$ when $k\rightarrow 0$, since both $\mathbf{v}_S$ and $\mathbf{v}^s_S$ vanish at large scales.

We then propose that, by tuning W^s such that $P_{\rm move}$ follows a form like Eq. D5, we could obtain the correct W^s and hence the correct $\mathbf{v}_\delta$ field. So far we still lack of a rigorous mathematical proof nor numerical verification for the above proposal. However, given its potential in reconstructing the 3D peculiar velocity in a less model dependent way, we hope to explore this possibility in future works.

---

[1] Y. Zheng and et al. (2012), in preparation.
[2] J. C. Jackson, MNRAS **156**, 1P (1972).
[3] W. L. W. Sargent and E. L. Turner, ApJL **212**, L3 (1977).
[4] P. J. E. Peebles, *The large-scale structure of the universe* (1980).
[5] N. Kaiser, MNRAS **227**, 1 (1987).
[6] J. A. Peacock and S. J. Dodds, MNRAS **267**, 1020 (1994), arXiv:astro-ph/9311057.
[7] W. E. Ballinger, J. A. Peacock, and A. F. Heavens, MNRAS **282**, 877 (1996), arXiv:astro-ph/9605017.
[8] J. A. Peacock, S. Cole, P. Norberg, C. M. Baugh, J. Bland-Hawthorn, T. Bridges, R. D. Cannon, M. Colless, C. Collins, W. Couch, et al., Nature (London) **410**, 169 (2001), arXiv:astro-ph/0103143.
[9] M. Tegmark, A. J. S. Hamilton, and Y. Xu, MNRAS **335**, 887 (2002), arXiv:astro-ph/0111575.
[10] M. Tegmark, M. R. Blanton, M. A. Strauss, F. Hoyle, D. Schlegel, R. Scoccimarro, M. S. Vogeley, D. H. Weinberg, I. Zehavi, A. Berlind, et al., Astrophys. J. **606**, 702 (2004), arXiv:astro-ph/0310725.
[11] L. Samushia, W. J. Percival, and A. Raccanelli, MNRAS **420**, 2102 (2012), 1102.1014.
[12] L. Guzzo, M. Pierleoni, B. Meneux, E. Branchini, O. Le Fèvre, C. Marinoni, B. Garilli, J. Blaizot, G. De Lucia, A. Pollo, et al., Nature (London) **451**, 541 (2008), 0802.1944.
[13] C. Blake, S. Brough, M. Colless, C. Contreras, W. Couch, S. Croom, T. Davis, M. J. Drinkwater, K. Forster, D. Gilbank, et al., MNRAS **415**, 2876 (2011), 1104.2948.

[14] C. Blake, S. Brough, M. Colless, C. Contreras, W. Couch, S. Croom, D. Croton, T. Davis, M. J. Drinkwater, K. Forster, et al., ArXiv e-prints (2012), 1204.3674.

[15] B. A. Reid, L. Samushia, M. White, W. J. Percival, M. Manera, N. Padmanabhan, A. J. Ross, A. G. Sánchez, S. Bailey, D. Bizyaev, et al., ArXiv e-prints (2012), 1203.6641.

[16] R. Tojeiro, W. J. Percival, J. Brinkmann, J. R. Brownstein, D. Eisenstein, M. Manera, C. Maraston, C. K. McBride, D. Duna, B. Reid, et al., ArXiv e-prints (2012), 1203.6565.

[17] L. Amendola, C. Quercellini, and E. Giallongo, MNRAS **357**, 429 (2005), arXiv:astro-ph/0404599.

[18] K. Yamamoto, B. A. Bassett, and H. Nishioka, Physical Review Letters **94**, 051301 (2005), arXiv:astro-ph/0409207.

[19] Y. Wang, JCAP **5**, 21 (2008), 0710.3885.

[20] W. J. Percival and M. White, MNRAS **393**, 297 (2009), 0808.0003.

[21] Y.-S. Song and W. J. Percival, JCAP **10**, 4 (2009), 0807.0810.

[22] M. White, Y.-S. Song, and W. J. Percival, MNRAS **397**, 1348 (2009), 0810.1518.

[23] Y.-S. Song, Phys. Rev. D **83**, 103009 (2011), 1009.2753.

[24] Y. Wang, W. Percival, A. Cimatti, P. Mukherjee, L. Guzzo, C. M. Baugh, C. Carbone, P. Franzetti, B. Garilli, J. E. Geach, et al., MNRAS **409**, 737 (2010), 1006.3517.

[25] P. Zhang, M. Liguori, R. Bean, and S. Dodelson, Physical Review Letters **99**, 141302 (2007), 0704.1932.

[26] B. Jain and P. Zhang, Phys. Rev. D **78**, 063503 (2008), 0709.2375.

[27] E. V. Linder, Astroparticle Physics **29**, 336 (2008), 0709.1113.

[28] R. Reyes, R. Mandelbaum, U. Seljak, T. Baldauf, J. E. Gunn, L. Lombriser, and R. E. Smith, Nature (London) **464**, 256 (2010), 1003.2185.

[29] Y.-C. Cai and G. Bernstein, MNRAS **422**, 1045 (2012), 1112.4478.

[30] E. Gaztañaga, M. Eriksen, M. Crocce, F. J. Castander, P. Fosalba, P. Marti, R. Miquel, and A. Cabré, MNRAS p. 2931 (2012), 1109.4852.

[31] E. Jennings, C. M. Baugh, B. Li, G.-B. Zhao, and K. Koyama, ArXiv e-prints (2012), 1205.2698.

[32] B. Li, W. A. Hellwing, K. Koyama, G.-B. Zhao, E. Jennings, and C. M. Baugh, ArXiv e-prints (2012), 1206.4317.

[33] H.-J. Seo and D. J. Eisenstein, Astrophys. J. **598**, 720 (2003), arXiv:astro-ph/0307460.

[34] D. J. Eisenstein, I. Zehavi, D. W. Hogg, R. Scoccimarro, M. R. Blanton, R. C. Nichol, R. Scranton, H.-J. Seo, M. Tegmark, Z. Zheng, et al., Astrophys. J. **633**, 560 (2005), arXiv:astro-ph/0501171.

[35] C. Blake, E. A. Kazin, F. Beutler, T. M. Davis, D. Parkinson, S. Brough, M. Colless, C. Contreras, W. Couch, S. Croom, et al., MNRAS **418**, 1707 (2011), 1108.2635.

[36] L. Anderson, E. Aubourg, S. Bailey, D. Bizyaev, M. Blanton, A. S. Bolton, J. Brinkmann, J. R. Brownstein, A. Burden, A. J. Cuesta, et al., ArXiv e-prints (2012), 1203.6594.

[37] E. V. Linder, Phys. Rev. D **72**, 043529 (2005), arXiv:astro-ph/0507263.

[38] D. Schlegel, F. Abdalla, T. Abraham, C. Ahn, C. Allende Prieto, J. Annis, E. Aubourg, M. Azzaro, S. B. C. Baltay, C. Baugh, et al., ArXiv e-prints (2011), 1106.1706.

[39] R. Laureijs, J. Amiaux, S. Arduini, J. . Augueres, J. Brinchmann, R. Cole, M. Cropper, C. Dabin, L. Duvet, A. Ealet, et al., ArXiv e-prints (2011), 1110.3193.

[40] U.-L. Pen, Astrophys. J. **504**, 601 (1998), arXiv:astro-ph/9711180.

[41] Y. P. Jing, H. J. Mo, and G. Boerner, Astrophys. J. **494**, 1 (1998), arXiv:astro-ph/9707106.

[42] R. Scoccimarro, Phys. Rev. D **70**, 083007 (2004), arXiv:astro-ph/0407214.

[43] U. Seljak and P. McDonald, JCAP **11**, 39 (2011), 1109.1888.

[44] T. Okumura, U. Seljak, P. McDonald, and V. Desjacques, JCAP **2**, 10 (2012), 1109.1609.

[45] T. Okumura, U. Seljak, and V. Desjacques, ArXiv e-prints (2012), 1206.4070.

[46] S. Bonoli and U. L. Pen, MNRAS **396**, 1610 (2009), 0810.0273.

[47] V. Desjacques and R. K. Sheth, Phys. Rev. D **81**, 023526 (2010), 0909.4544.

[48] A. J. S. Hamilton and M. Culhane, MNRAS **278**, 73 (1996), arXiv:astro-ph/9507021.

[49] X. Kang, Y. P. Jing, H. J. Mo, and G. Börner, MNRAS **336**, 892 (2002), arXiv:astro-ph/0201124.

[50] A. F. Heavens, S. Matarrese, and L. Verde, MNRAS **301**, 797 (1998), arXiv:astro-ph/9808016.

[51] T. Matsubara, Phys. Rev. D **77**, 063530 (2008), 0711.2521.

[52] T. Matsubara, Phys. Rev. D **78**, 083519 (2008), 0807.1733.

[53] A. Taruya, T. Nishimichi, and S. Saito, Phys. Rev. D **82**, 063522 (2010), 1006.0699.

[54] T. Matsubara, Phys. Rev. D **83**, 083518 (2011), 1102.4619.

[55] T. Okamura, A. Taruya, and T. Matsubara, JCAP **8**, 12 (2011), 1105.1491.

[56] M. Sato and T. Matsubara, Phys. Rev. D **84**, 043501 (2011), 1105.5007.

[57] M. White, MNRAS **321**, 1 (2001), arXiv:astro-ph/0005085.

[58] U. Seljak, MNRAS **325**, 1359 (2001), arXiv:astro-ph/0009016.

[59] J. L. Tinker, D. H. Weinberg, and Z. Zheng, MNRAS **368**, 85 (2006), arXiv:astro-ph/0501029.

[60] J. L. Tinker, MNRAS **374**, 477 (2007), arXiv:astro-ph/0604217.

[61] K. B. Fisher, Astrophys. J. **448**, 494 (1995), arXiv:astro-ph/9412081.

[62] B. A. Reid and M. White, MNRAS **417**, 1913 (2011), 1105.4165.

[63] T. Okumura and Y. P. Jing, Astrophys. J. **726**, 5 (2011), 1004.3548.

[64] E. Jennings, C. M. Baugh, and S. Pascoli, MNRAS **410**, 2081 (2011), 1003.4282.

[65] J. Kwan, G. F. Lewis, and E. V. Linder, Astrophys. J. **748**, 78 (2012), 1105.1194.

[66] E. Jennings, C. M. Baugh, and S. Pascoli, ApJL **727**, L9 (2011), 1011.2842.

[67] D. Bianchi, L. Guzzo, E. Branchini, E. Majerotto, S. de la Torre, F. Marulli, L. Moscardini, and R. E. Angulo, ArXiv e-prints (2012), 1203.1545.

[68] S. de la Torre and L. Guzzo, ArXiv e-prints (2012), 1202.5559.

[69] F. Bernardeau, S. Colombi, E. Gaztañaga, and R. Scoccimarro, Physics reports **367**, 1 (2002), arXiv:astro-ph/0112551.

[70] S. Pueblas and R. Scoccimarro, Phys. Rev. D **80**, 043504 (2009), 0809.4606.

[71] B. Jain and J. Khoury, Annals of Physics **325**, 1479 (2010), 1004.3294.

[72] T. Clifton, P. G. Ferreira, A. Padilla, and C. Skordis, Physics reports **513**, 1 (2012), 1106.2476.

[73] A. Cooray and R. Sheth, Physics reports **372**, 1 (2002), arXiv:astro-ph/0206508.

[74] X. Yang, H. J. Mo, and F. C. van den Bosch, MNRAS **339**, 1057 (2003), arXiv:astro-ph/0207019.

[75] Z. Zheng, A. A. Berlind, D. H. Weinberg, A. J. Benson, C. M. Baugh, S. Cole, R. Davé, C. S. Frenk, N. Katz, and C. G. Lacey, Astrophys. J. **633**, 791 (2005), arXiv:astro-ph/0408564.

[76] T. Hamana, I. Kayo, N. Yoshida, Y. Suto, and Y. P. Jing, MNRAS **343**, 1312 (2003), arXiv:astro-ph/0305187.

[77] R. K. Sheth and A. Diaferio, MNRAS **322**, 901 (2001), arXiv:astro-ph/0009166.

[78] L. Lombriser, Phys. Rev. D **83**, 063519 (2011), 1101.0594.

[79] R. A. Sunyaev and I. B. Zeldovich, MNRAS **190**, 413 (1980).

[80] N. Hand, G. E. Addison, E. Aubourg, N. Battaglia, E. S. Battistelli, D. Bizyaev, J. R. Bond, H. Brewington, J. Brinkmann, B. R. Brown, et al., ArXiv e-prints (2012), 1203.4219.

[81] J. Dunkley, R. Hlozek, J. Sievers, V. Acquaviva, P. A. R. Ade, P. Aguirre, M. Amiri, J. W. Appel, L. F. Barrientos, E. S. Battistelli, et al., Astrophys. J. **739**, 52 (2011), 1009.0866.

[82] E. Shirokoff, C. L. Reichardt, L. Shaw, M. Millea, P. A. R. Ade, K. A. Aird, B. A. Benson, L. E. Bleem, J. E. Carlstrom, C. L. Chang, et al., Astrophys. J. **736**, 61 (2011), 1012.4788.

[83] C. L. Reichardt, L. Shaw, O. Zahn, K. A. Aird, B. A. Benson, L. E. Bleem, J. E. Carlstrom, C. L. Chang, H. M. Cho, T. M. Crawford, et al., ArXiv e-prints (2011), 1111.0932.

[84] S. Ho, S. Dedeo, and D. Spergel, ArXiv e-prints (2009), 0903.2845.

[85] J. Shao, P. Zhang, W. Lin, Y. Jing, and J. Pan, MNRAS **413**, 628 (2011), 1004.1301.

[86] Strictly speaking, the decomposition only guarantees $\langle \delta\theta_S \rangle = 0$. To reach $P_{g\theta_S} = 0$ requires that a velocity component uncorrelated with the matter density field should be uncorrelated with the galaxy distribution. This is an issue to be investigated in future works.